Review

Not peer-reviewed version

A Review of Reduced-Order Modeling of PCM-Based Latent Heat Storage Systems

John Nico Omlang * and Aldrin Calderon

Posted Date: 28 February 2026

doi: 10.20944/preprints202602.1504.v1

Keywords: reduced-order modeling; latent heat storage; phase change materials; thermal energy storage; proper orthogonal decomposition; machine learning; heat exchanger; data-driven modeling; CFD model reduction

 doi:10.20944/preprints202602.1504.v1

Review

A Review of Reduced-Order Modeling of PCM-Based Latent Heat Storage Systems

John Nico Omlang [1,2,3,*] and Aldrin Calderon [1,2]

[1] School of Mechanical, Manufacturing, and Energy Engineering, Mapua University, Manila, Philippines
[2] School of Graduate Studies, Mapua University, Manila, Philippines
[3] Mechanical Engineering Department, Far Eastern University Institute of Technology, Manila, Philippines
* Correspondence: jnomlang@feutech.edu.ph

Abstract

Phase change material (PCM)-based latent heat storage (LHS) systems help address the mismatch between renewable energy supply and thermal demand. However, their practical implementation is constrained by the strongly nonlinear and multiphysics nature of phase change, which makes high-fidelity simulations and real-time applications computationally expensive. This review examines Reduced-Order Modeling (ROM) as an effective strategy to overcome this limitation by combining physics-based simplifications, projection methods, interpolation techniques, and data-driven models for PCM-based LHS systems. The review covers approaches such as two-temperature non-equilibrium and analytical thermal-resistance models, Proper Orthogonal Decomposition (POD), CFD-derived look-up tables, kriging and ε-NTU grey/black-box metamodels, and machine-learning methods including artificial neural networks and gradient-boosted regressors trained from CFD data. These ROM techniques have been applied to packed beds, PCM-integrated heat exchangers, finned enclosures, triplex-tube systems, and solar thermal components, achieving speed-ups from tens to over 80,000 times faster than full CFD simulations while maintaining prediction errors typically below 5% or within sub-Kelvin temperature deviations. A critical comparative analysis exposes the fundamental trade-off between interpretability, data dependence, and computational efficiency, guiding method selection for specific applications. Remaining challenges include accurate representation of phase-change nonlinearity, moving phase boundaries, multi-timescale dynamics, generalizability across geometries, and integration into system-level frameworks, motivating future hybrid physics–machine learning developments and standardization efforts.

Keywords: reduced-order modeling; latent heat storage; phase change materials; thermal energy storage; proper orthogonal decomposition; machine learning; heat exchanger; data-driven modeling; CFD model reduction

1. Introduction

The global shift toward sustainable energy systems has placed unprecedented demand on energy storage technologies as societies confront the twin challenges of climate change and energy security. Among the available options, thermal energy storage (TES) has emerged as a key enabling technology for improving the use of renewable energy sources, particularly in addressing the intermittent nature of solar and wind power [1]. Among various TES approaches, latent heat storage (LHS) systems employing phase change materials (PCMs) have garnered significant attention due to their ability to store and release substantial amounts of thermal energy within narrow temperature ranges. These systems offer compelling advantages over sensible heat storage, including higher energy storage density, isothermal operation during phase transitions, and reduced system volume requirements [2]. The applications of PCM-based LHS span diverse sectors, from solar thermal power generation and building temperature regulation to electronic device cooling and industrial waste heat recovery [3].

 doi:10.20944/preprints202602.1504.v1

Despite their promising potential, PCM-based LHS systems face substantial challenges that hinder their widespread adoption and optimal design. The most significant limitation stems from the inherently low thermal conductivity of most organic and inorganic PCMs, typically ranging from 0.2 to 0.3 W/m·K, which leads to prolonged charging and discharging times and reduced overall system efficiency [2]. This thermal transport bottleneck creates strong physical non-linearities and geometric discontinuities during phase transitions, making accurate numerical prediction of system behavior exceedingly complex [4]. Traditional approaches to address these challenges include geometric enhancements such as fins and extended surfaces [5], encapsulation strategies to prevent material leakage while enhancing heat transfer [6], and incorporation of high-conductivity nanoparticles or porous structures [7]. However, each enhancement technique introduces additional complexity to the modeling and simulation framework, compounding the computational burden required for accurate system characterization.

The mathematical modeling of phase change processes in LHS systems presents formidable computational challenges. Two primary approaches exist for formulating phase change problems: front-tracking methods that explicitly determine the position of the two-phase interface at each time step, and fixed-grid methods such as the enthalpy-porosity approach that treat the phase change as a continuum problem without explicit interface tracking [2]. While front-tracking methods work well for simple Stefan problems, they prove poorly suited for real-world applications involving complex geometries, natural convection, and multiple heat sources [1]. Consequently, researchers predominantly employ enthalpy-based finite element method (FEM) or finite volume method (FVM) simulations coupled with models such as the Lee model for phase change kinetics [8]. These high-fidelity full-order models (FOMs) impose severe computational penalties even though they provide detailed spatial and temporal resolution of temperature fields, liquid fraction evolution, and flow patterns. Simulations of even moderately sized LHS systems can require days or weeks to complete on modern workstations [9], making iterative design optimization, parametric studies, and real-time control applications effectively intractable. This computational bottleneck becomes particularly acute when considering system-level analyses that require thousands of simulations runs to characterize performance across varying operating conditions, material properties, and geometric configurations [1].

The necessity to balance computational accuracy with engineering practicality has driven the development of reduced-order modeling (ROM) techniques specifically tailored for PCM-based LHS systems. These methodologies aim to capture the essential physics of phase change heat transfer while dramatically reducing the number of degrees of freedom and computational time required for simulation. Several distinct ROM approaches have emerged in the literature, each with particular strengths and limitations. Proper Orthogonal Decomposition (POD), originally proposed by Lumley in 1967 for turbulence analysis [8], exemplifies one such approach and has been successfully adapted to LHS applications, as detailed in Section 3.1.1. Recent implementations have demonstrated computational speedups exceeding 300-fold while maintaining temperature prediction errors below 0.1% [8]. Alternative approaches include effectiveness-Number of Transfer Units (ε-NTU) methods that characterize thermal resistance between heat transfer fluid and phase change boundaries through empirical correlations [1], and one-dimensional analytical models based on simplified radial conduction assumptions suitable for specific geometric configurations such as cylindrical capsules [2].

An emerging and particularly promising direction involves CFD-informed reduced-order models that leverage detailed computational fluid dynamics simulations to construct look-up tables or surrogate functions describing capsule-level behavior, which are then implemented in fast system-level models. This hierarchical approach enables temporal mean deviations in energy content predictions as low as 5% with simulation times reduced from weeks to seconds [9]. Furthermore, the integration of machine learning techniques with traditional ROM frameworks has opened new avenues for rapid thermal field prediction and design optimization. Hybrid methodologies combining POD with artificial neural networks, radial basis functions, or Gaussian process regression

 doi:10.20944/preprints202602.1504.v1

have demonstrated the ability to predict PCM heat exchanger performance across wide parameter ranges with mean absolute deviations in outlet temperatures below 0.1 K. Black-box and grey-box models utilizing kriging, response surface methods, or deep learning architectures provide system simulation speedup ratios ranging from 11 to 57 compared to full-order models, while maintaining accuracy penalties below 3% for key performance metrics such as compressor energy consumption and total charging time [1].

Despite these advances, significant controversies and unresolved questions persist within the ROM community for LHS applications. A fundamental tension exists between model fidelity and computational efficiency, with researchers adopting divergent philosophies regarding acceptable trade-offs. Some studies emphasize purely data-driven approaches that prioritize speed and flexibility but may lack physical consistency or interpretability, while others advocate for physics-informed methods that embed governing equations into the reduced-order framework to ensure thermodynamic plausibility [10]. The question of how much geometric and physical detail must be retained in reduced models remains debatable. For instance, recent investigations have questioned whether capsule walls and heat transfer fluid domains must be explicitly included in CFD models used to generate ROM training data, with evidence suggesting that properly defined convective boundary conditions may suffice for certain applications [9]. Similarly, the optimal approach for handling nonlinearities inherent to phase change processes—whether through empirical correlations, discrete empirical interpolation, or neural network approximations—continues to generate debate [2]. The generalizability of ROM across different operating regimes, geometric configurations, and PCM types presents another critical challenge, as models trained on specific datasets may exhibit degraded performance when extrapolated beyond their training domains [1].

This review aims to provide a comprehensive and critical assessment of the state-of-the-art in reduced-order modeling techniques for PCM-based LHS systems. We systematically examine the theoretical foundations, implementation methodologies, validation approaches, and performance characteristics of major ROM categories including POD-based projection methods, analytical reduced models, CFD-informed surrogate models, and machine learning-enhanced frameworks. Particular attention is devoted to quantitative comparisons of computational efficiency gains versus accuracy penalties, identification of application-specific suitability of different ROM approaches, and delineation of current limitations and future research directions. By synthesizing findings from over 40 relevant studies spanning thermal engineering, computational mathematics, and data science, this review establishes that properly constructed reduced-order models can achieve computational speedups of 2-3 orders of magnitude while maintaining prediction errors below 10% for most practical applications. However, we also highlight that significant work remains to develop robust, generalizable ROM frameworks capable of handling the full complexity of real-world LHS systems across diverse operating conditions, and to establish standardized validation protocols that enable fair comparison across different modeling approaches. This review thereby provides both a foundation for researchers entering the field and a roadmap for advancing ROM capabilities to enable the next generation of optimized, intelligently controlled PCM-based thermal energy storage systems.

This review aims to provide a comprehensive and critical assessment of the state-of-the-art in reduced-order modeling techniques for PCM-based LHS systems. The objectives are threefold: (1) to categorize and critically evaluate ROM methodologies applicable to PCM-based LHS systems, (2) to synthesize reported performance metrics and speed-up factors through comparative case study analysis, and (3) to identify persistent challenges and chart future research directions. The review is organized as follows. Section 2 provides background on common LHS configurations and the governing physics that motivate ROM development. Section 3 presents a taxonomic classification of ROM methods—physics-based, projection-based, and data-driven—with attention to their underlying assumptions and suitability for phase-change problems. Section 4 discusses the advantages of ROMs in LHS applications alongside configuration-specific challenges including nonlinearity, moving boundaries, and multi-timescale dynamics. Section 5 examines representative

 doi:10.20944/preprints202602.1504.v1

case studies drawn from the literature, comparing methodologies, accuracy, and computational speed-up. Section 6 synthesizes remaining challenges and proposes future research directions, emphasizing hybrid physics-machine learning approaches and the need for standardized validation. Conclusions are presented in Section 7.

2. Overview of PCM-Based Latent Heat Storage (LHS) Systems

Latent heat storage (LHS) systems have emerged as a key technology for enhancing thermal energy management in various industrial and renewable energy applications. These systems exploit the high energy density associated with phase change processes, enabling efficient storage and release of thermal energy within relatively compact volumes. Among the different approaches, configurations based on PCMs are particularly attractive due to their ability to maintain nearly constant temperature during melting and solidification. The design and arrangement of PCM-based systems significantly influence heat transfer performance, system efficiency, and scalability.

2.1. Common PCM-Based Latent Heat Storage Configurations

2.1.1. Shell-and-Tube Systems

The standard shell-and-tube design for LHS systems consists of PCM occupying the shell side, while heat transfer fluid (HTF) flows through internal tubes. This configuration offers a practical balance between simplicity and scalability. However, its performance is limited by the inherently low thermal conductivity of PCM [11,12]. To address this limitation, multiple PCMs with different melting temperatures can be staged within the system, improving heat transfer uniformity. Studies have shown that using three cascaded PCM units enhances latent heat utilization and system effectiveness by approximately 15–20% compared to single-PCM systems [11]. Another widely adopted enhancement involves the integration of finned tubes, which increases the effective heat transfer surface area and accelerates the phase change process. Experimental results indicate that finned designs can reduce solidification time by 30–40%, significantly improving overall thermal performance [13].

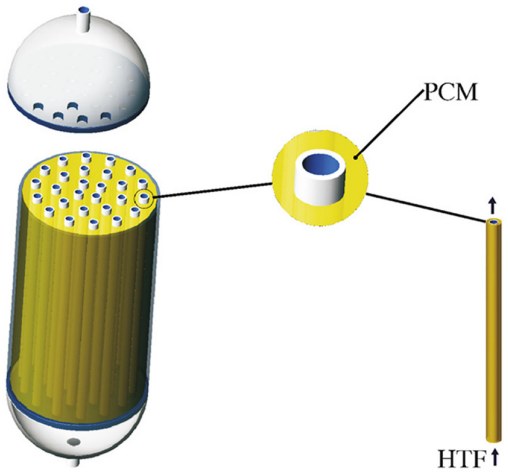

Figure 1. Shell-and-tube thermal energy storage [12].

2.1.2. Triplex-Tube (Triple-Tube) Systems

Triplex-tube heat exchangers (TTHE) represent an advanced configuration for thermal energy storage systems. These designs employ concentric tubes, where the inner and outer tubes circulate heat transfer fluid (HTF), while the intermediate tube contains the PCM. This arrangement enables simultaneous heat storage and release along with direct hot water supply [14]. To enhance thermal performance, geometric optimization of the inner tube has been explored. Non-circular shapes such

 doi:10.20944/preprints202602.1504.v1

as square or pentagonal profiles showed significant improvement in heat transfer. For instance, square tubes have been shown to reduce solidification time by approximately 25% compared to conventional circular designs, primarily due to their increased surface area [15]. Furthermore, the incorporation of cascaded PCMs maintains a favorable thermal gradient throughout the system. This approach has demonstrated improvements in exergy efficiency ranging from 12% to 18% using materials such as RT35, RT50, and RT60 [16,17].

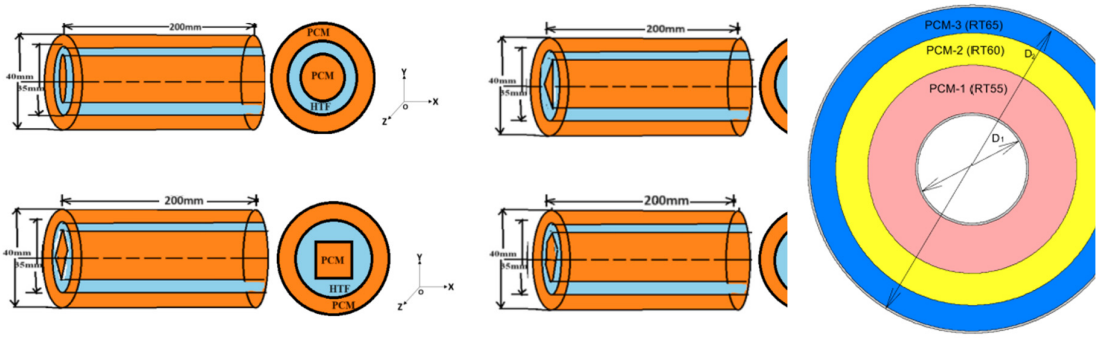

(**a**) (**b**)

Figure 2. Triplex-tube LHS systems. (a) Triplex-tube LHS with PCM in the intermediate tube [15]; (b) Triplex-tube LHS with multiple concentric PCMs [16].

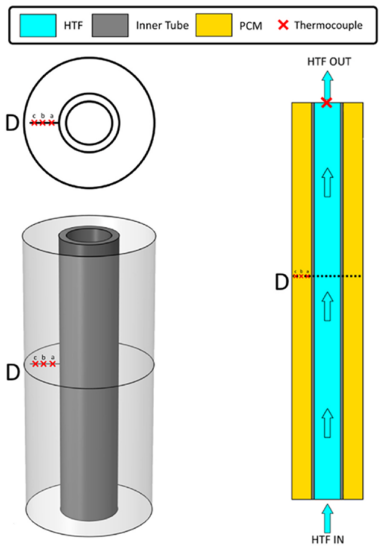

Figure 3. Double-tube LHS configuration [18].

2.1.3. Double-Tube (Concentric Pipe) Systems

Double-tube configurations employ two concentric pipes with PCM typically surrounding an inner tube through which HTF flows. While more traditional than triplex-tube designs, these systems remain common for applications like domestic water heating and solar thermal systems [18].

2.1.4. Plate Heat Exchanger (PHE) Systems

Plate-based configurations represent an alternative geometry where PCM is enclosed between parallel metal plates, with HTF flowing through channels. These systems offer a massive heat transfer surface within a compact design [19]. Variants include:

 doi:10.20944/preprints202602.1504.v1

- Corrugated plate designs: Using herringbone profiles for enhanced contact [20]
- Roll-bonded plate systems: PCM is stored in a vessel and HTF flows through roll-bonded plates [19]
- Flat-plate configurations: Simplified geometries with parallel HTF channels separated by PCM volumes [21]

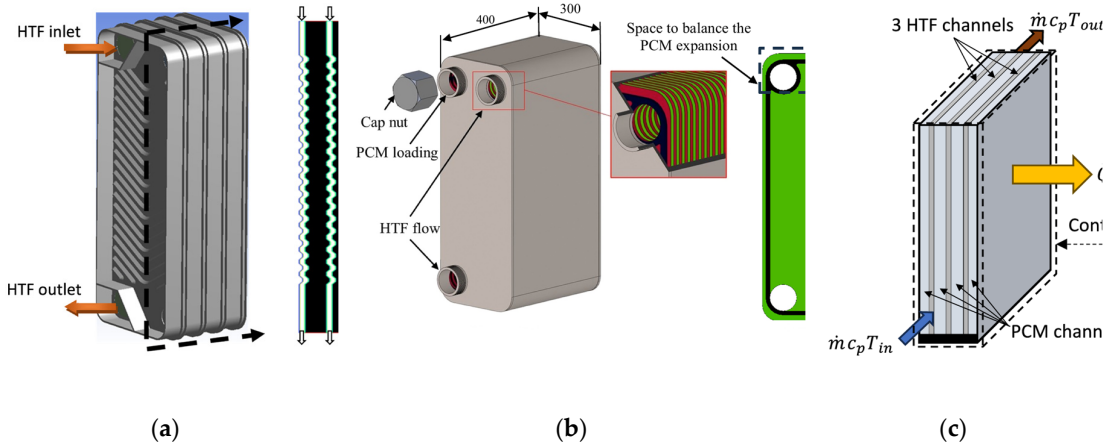

Figure 4. Different PHE systems. (**a**) Corrugated PHE-LHS system [20]; (**b**) Roll-bonded PHE-LHS systems [19]; (**c**) Flat-plate PHE-LHS system [21].

2.1.5. Packed-Bed Systems

These configurations store PCM in encapsulated forms randomly packed within a tank, with HTF flowing through the bed. The advantage is increased heat transfer area through capsule encapsulation [22]. Modern variants include systems with ordered arrangements to control HTF flow distribution and improve performance uniformity [22].

Figure 5. Encapsulated PCM in flexible pouches stacked in a LHS tank [22].

The diversity of configurations illustrated above—shell-and-tube, triplex-tube, plate, and encapsulated systems—shares a common underlying physics: transient heat transfer with solid-liquid phase change. Understanding this physics is essential for appreciating why reduced-order modeling is both necessary and challenging. The following subsection presents the governing equations that describe these systems and the numerical methods used to solve them at full order, providing the foundation for the ROM techniques surveyed in Section 3.

 doi:10.20944/preprints202602.1504.v1

2.2. Physical and Numerical Modeling of PCM-Based LHS System

Reduced-order modeling of LHS systems is fundamentally grounded in the mathematical and numerical description of phase-change heat transfer. Most ROMs reported in the literature are derived from, trained on, or validated against high-fidelity numerical simulations that resolve transient melting and solidification processes of PCMs. A brief discussion of the governing equations and numerical solution strategies commonly employed in PCM-based LHS modeling are presented in the next subsections to contextualize the structure, complexity, and limitations of existing ROM approaches.

2.2.1. Governing Equations for Phase-Change Heat Transfer

The thermal behavior of PCM-based LHS systems is primarily governed by the conservation of energy, with phase change introducing strong nonlinearities through latent heat effects. For most engineering applications, the energy equation is expressed in an enthalpy-based form, which allows both sensible and latent heat contributions to be treated within a unified framework [23,24].

In the absence of volumetric heat generation, the transient energy equation for a PCM domain can be written as

$$\rho \frac{\partial h}{\partial t} + \rho \mathbf{u} \cdot \nabla h = \nabla \cdot (k \nabla T), \tag{1}$$

where ρ is the density, h is the specific enthalpy, $\mathbf{u}$ is the velocity vector, k is the thermal conductivity, and T is the temperature. In purely conductive PCM systems, the convective term vanishes ($\mathbf{u} = 0$), while in convection-enhanced systems the energy equation is coupled with the momentum equations.

The enthalpy-temperature relationship accounts for latent heat storage through the introduction of a liquid phase fraction f_l, commonly expressed as

$$h = c_p T + f_l L, \tag{2}$$

where c_p is the specific heat capacity and L is the latent heat of fusion. The liquid fraction varies between zero and unity and is typically defined as a function of temperature over a finite melting interval to ensure numerical stability [25].

The nonlinear coupling between temperature and phase fraction introduces a moving solid-liquid interface, which is the defining feature of PCM-based LHS systems. This nonlinearity significantly increases the dimensionality and stiffness of the resulting discretized system and poses a major challenge for reduced-order modeling.

In configurations where natural or forced convection within the molten PCM is important, the energy equation is coupled with the incompressible Navier–Stokes equations through buoyancy-driven flow, often modeled using the Boussinesq approximation [26]. However, many ROM studies focus on conduction-dominated configurations or treat convective effects in a simplified manner to reduce computational complexity.

2.2.2. Numerical Methods for High-Fidelity PCM Simulations

Several numerical methods have been developed to solve the governing equations of phase-change heat transfer. Among these, the enthalpy–porosity method is the most widely used approach for simulating melting and solidification in PCM-based LHS systems [25,27]. In this method, PCM is treated as a porous medium in the mushy zone, with the liquid fraction acting as a porosity parameter that controls momentum damping in the partially molten region. This approach eliminates the need for explicit interface tracking and is therefore well suited for complex geometries.

An alternative formulation is the effective heat capacity method, in which the latent heat is incorporated into an augmented heat capacity over the phase-change temperature range [28]. While computationally attractive, this method may suffer from numerical diffusion and reduced accuracy when sharp phase fronts are present.

 doi:10.20944/preprints202602.1504.v1

High-fidelity PCM simulations are commonly discretized using the finite volume or finite element methods, combined with implicit time integration schemes to ensure numerical stability during rapid phase transitions [29]. Accurate resolution of steep temperature gradients near the phase interface typically requires fine spatial discretization, leading to large-scale systems of algebraic equations. As a result, transient simulations of charging and discharging cycles are computationally expensive, especially when multiple operating conditions or geometric parameters are considered.

From a reduced-order modeling standpoint, these numerical formulations give rise to FOMs characterized by:

- high state dimensionality,
- strong nonlinearities due to phase change,
- long transient simulation horizons, and
- sensitivity to operating and geometric parameters.

These features directly influence the design and performance of ROM techniques applied to PCM-based LHS systems.

2.2.3. Implications for Model Order Reduction

The governing equations and numerical formulations described above present several challenges for reduced-order modeling. First, the nonlinear enthalpy–temperature relationship and the presence of a moving phase boundary violate the linearity assumptions underlying classical projection-based ROMs, such as Proper Orthogonal Decomposition (POD)–Galerkin methods [30]. Consequently, a large number of modes may be required to accurately represent the system dynamics, particularly during rapid melting or solidification stages. Second, the strong dependence of PCM behavior on geometry, boundary conditions, and operating parameters limits the generalizability of ROMs trained for a specific configuration. This issue is particularly pronounced in finned or convection-enhanced LHS systems, where spatial complexity increases the effective dimensionality of the solution manifold. Finally, the multi-timescale and highly transient nature of PCM charging and discharging processes imposes stringent requirements on ROM stability and long-term accuracy. For applications such as real-time control, optimization, and digital twins, ROMs must remain robust across extended simulation horizons and varying operating conditions.

These features—high state dimensionality, strong nonlinearities, long transient horizons, and parameter sensitivity—directly influence ROM design. For example, the nonlinear enthalpy-temperature relationship violates the linearity assumptions underlying classical POD-Galerkin methods (Section 3.1.1), motivating nonlinear techniques such as Discrete Empirical Interpolation Method (DEIM) (Section 3.2.1). Similarly, the dependence on geometry and boundary conditions limits the generalizability of data-driven surrogates (Section 3.3) trained for specific configurations. The multi-timescale behavior discussed in Section 4.2.3 imposes stringent requirements on ROM stability over extended simulation horizons, favoring methods that preserve long-term energy conservation.

3. Common Reduced-Order Modeling Methods

Reduced-order models (ROMs) are essential tools for simplifying complex, high-dimensional dynamical systems while preserving their essential characteristics, which is crucial for computational efficiency and analysis across various scientific and engineering disciplines [31–33]. The development of ROMs aims to bridge the gap between high-fidelity simulations, which can be computationally expensive and time-consuming, and the need for rapid analysis, optimization, and real-time control [33,34]. This is particularly relevant in fields like computational fluid dynamics (CFD), structural mechanics, and control systems [35,36]. The methodologies can be broadly categorized into projection-based linear ROMs. The following subsections detail each approach, with attention to their mathematical foundations, offline/online workflows, and inherent strengths and weaknesses.

 doi:10.20944/preprints202602.1504.v1

3.1. Projection-Based Linear ROMs

Projection-based ROMs leverage linear subspaces to approximate system dynamics, relying on techniques like Proper Orthogonal Decomposition (POD) or a predefined basis.

3.1.1. Proper Orthogonal Decomposition (POD)-Galerkin

One of the most widely recognized and frequently applied techniques for model order reduction is Proper Orthogonal Decomposition (POD)-Galerkin [37–44]. The POD-Galerkin method constructs a reduced basis by identifying dominant spatial modes from a set of high-fidelity simulation snapshots [45,46]. These modes, ordered by their energy content, form an orthonormal basis that captures most of the system's variance with a significantly smaller number of vectors than the original full-order model (FOM) [45]. The system's governing equations (e.g., Navier-Stokes equations) are then projected onto this low-dimensional subspace using a Galerkin projection, leading to a reduced system of ordinary differential equations [46]. This projection preserves the physical structure of the original equations to some extent [47].

The mathematical basis of POD-Galerkin ROMs typically involves a structured workflow comprising offline and online phases [48,49]. In the offline phase, a set of snapshots (solutions from the FOM at different time instances or parameter values) is generated. POD is then applied to these snapshots to extract the dominant modes, which constitute the reduced basis. The FOM equations are projected onto this basis to derive the reduced-order system. In the online phase, the precomputed reduced-order system is solved rapidly for new parameters or time steps, yielding low-dimensional coefficients that are then mapped back to the high-dimensional physical space using the established POD modes [45,46].

POD-Galerkin ROMs are computationally efficient once the offline phase is complete, making them suitable for real-time applications and rapid parameter exploration [50]. They offer a physically consistent reduction, as the Galerkin projection maintains some connection to the underlying physics[47]. The method is particularly effective for systems with coherent structures or dominant modes [51]. Their performance can degrade significantly for highly nonlinear systems or systems with propagating fronts and shocks, as linear subspaces struggle to capture these features effectively [52]. The offline phase can be computationally expensive due to the need for FOM simulations and singular value decomposition (SVD) for POD basis generation [45]. Closure modeling is often required for nonlinear terms to account for the truncated modes' influence, which can be complex [45,53].

3.1.2. Reduced Basis (RB)

The Reduced Basis method aims to construct a low-dimensional subspace that spans the solution manifold of a parametric partial differential equation (PDE) [54]. Unlike POD, which is purely data-driven, RB methods typically involve a greedy sampling approach to select basis vectors from a collection of solutions (snapshots) that are generated for different parameter instances [54,55]. The criterion for selecting snapshots often involves an a posteriori error estimator, ensuring that the chosen basis effectively approximates the solution across the entire parameter space. The FOM is then projected onto this basis [54].

The workflow of RB consists of offline and online phase. The offline stage involves a parameter space exploration. A series of FOM solutions are computed for various parameter values. A greedy algorithm iteratively selects parameter instances whose corresponding FOM solutions maximally enrich the reduced basis, typically guided by an error estimator. This process generates a compact, parameter-dependent reduced basis. In the online stage, for new parameter values, the precomputed reduced operators are used to solve the reduced-order system, providing a fast and accurate approximation of the FOM solution [54,55].

 doi:10.20944/preprints202602.1504.v1

RB methods provide rigorous error bounds, which are crucial for certified real-time simulations and design optimization. They are well-suited for parametric PDEs, offering rapid evaluation for new parameter queries [54]. The greedy approach ensures an efficient and optimal basis selection [55].

Developing reliable and efficient error estimators can be challenging for complex problems, especially those with non-affine parameter dependencies [54]. The offline training can still be very time-consuming, particularly for high-dimensional parameter spaces [55]. Nonlinear problems often require hyper-reduction techniques to alleviate computational bottlenecks [47].

3.1.3. Proper Generalized Decomposition (PGD)

Proper Generalized Decomposition (PGD) is a model reduction technique that approximates high-dimensional solutions as a finite sum of separable functions, where each function is a product of univariate functions, typically one for each independent variable (e.g., spatial coordinates, time, and parameters) [56–58]. This separated representation drastically reduces the dimensionality of the problem by transforming a single high-dimensional problem into a series of coupled one-dimensional problems [59].

The offline phase of this method involves an iterative construction of the separable functions [56,57]. Starting with an initial guess, a fixed-point iteration or greedy algorithm computes one pair of functions (e.g., a spatial function and a parameter function) at a time, until a desired accuracy is reached [56]. This process is inherently "online" in the sense that once the separated representation is built, the solution for any combination of parameters or time can be evaluated directly without solving new systems [58].

PGD intrinsically handles high-dimensional parametric and multi-physical problems, often referred to as "curse of dimensionality" issues, by avoiding full tensor product spaces [56,58]. It produces a parameterized solution in a single offline computation, which can then be evaluated very rapidly for any parameter in the online phase [58]. PGD can also be applied to eigenvalue problems [59].

3.2. Nonlinear and Hyper-Reduced ROMs

The projection-based linear ROMs discussed in Section 3.1, while powerful, face fundamental limitations when applied to the strongly nonlinear governing equations such as that of PCM phase change (see Section 2.2). Their computational efficiency is eroded because evaluating nonlinear terms (e.g., in the enthalpy-temperature relationship) still requires operations scaling with the high-dimensional FOM. To overcome this, hyper-reduction techniques such as the Discrete Empirical Interpolation Method (DEIM) and Gauss-Newton with Approximated Tensors (GNAT) have been developed. These methods approximate nonlinear terms by evaluating them only at a strategically selected subset of points, thereby preserving the speed advantage of the ROM.

3.2.1. Discrete Empirical Interpolation Method (DEIM)

Discrete Empirical Interpolation Method (DEIM) is a hyper-reduction technique used to efficiently approximate nonlinear terms in projection-based ROMs, typically in conjunction with POD-Galerkin or RB methods [52,60]. The core idea is to approximate a high-dimensional nonlinear function using a small subset of its components (or "magic points") and a corresponding empirical basis [61]. This avoids evaluating the nonlinear term over the entire high-dimensional domain, significantly reducing computational cost [60].

In the offline stage of this method, snapshots of the nonlinear term are collected, and an empirical basis for this term is constructed. DEIM then identifies a subset of "magic points" (spatial locations) where the nonlinear term needs to be evaluated. An interpolation matrix is also constructed. In the online stage, only the values of the nonlinear term at these magic points are computed, and the full nonlinear term is approximated using the precomputed empirical basis and interpolation matrix [60,62].

 doi:10.20944/preprints202602.1504.v1

DEIM effectively alleviates the computational burden associated with nonlinear terms in ROMs, making projection-based ROMs feasible for many nonlinear problems [60,63]. It provides a systematic way to select sparse sensor locations [64].

The accuracy of DEIM depends heavily on the choice of magic points and the quality of the empirical basis, which can be sensitive to the problem's characteristics [60,61]. The offline phase to construct the DEIM basis and select magic points can still be costly [64]

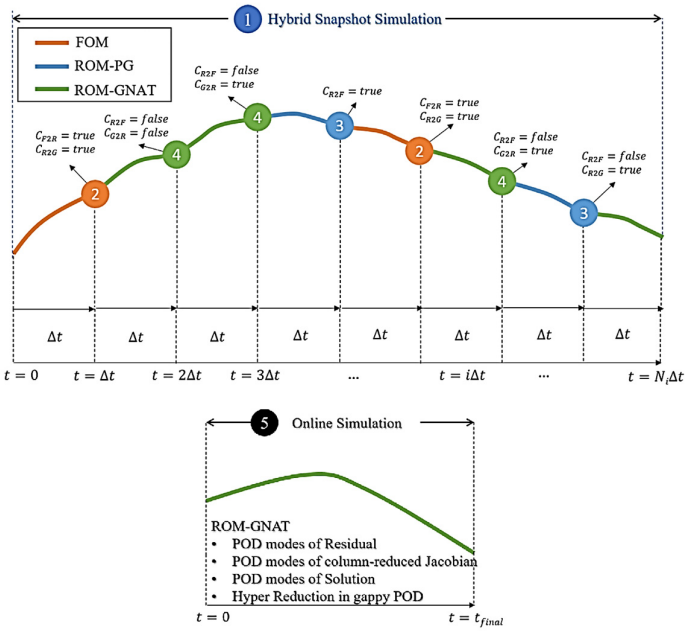

Figure 6. Development of a GNAT-embedded hybrid snapshot approach and formulation of ROM-GNAT for online simulation [65].

3.2.2. Gauss-Newton with Approximated Tensors (GNAT)

Gauss-Newton with Approximated Tensors (GNAT) is another hyper-reduction technique specifically designed to accelerate the solution of nonlinear reduced-order systems. It leverages the Gauss-Newton method for solving the nonlinear system, but crucially, it approximates the Jacobian and residual tensors by interpolating them at a reduced set of "collocation points" rather than computing them over the entire domain [65]. This approach is often combined with POD for basis generation [63].

The offline phase involves generating snapshots and constructing a POD basis for the solution. Additionally, snapshots of the nonlinear residual and its Jacobian are used to form reduced bases for these quantities. GNAT then identifies a set of optimal collocation points, similar to DEIM, where the nonlinear residual and Jacobian components are evaluated [63,65]. In the online phase, the nonlinear reduced-order system is solved using an iterative Gauss-Newton scheme, where the residual and Jacobian are approximated by evaluating them only at the pre-selected collocation points, leading to significant speed-ups. Figure 6 illustrates a hybrid snapshot simulation which can embed GNAT for enhanced generation speed [65].

GNAT is highly effective in accelerating nonlinear ROMs, offering significant computational savings compared to full-order Gauss-Newton iterations [63,65]. It maintains good accuracy by directly approximating the terms relevant to the nonlinear solver. GNAT can be embedded into hybrid snapshot simulations to improve efficiency and representation [65]. Like DEIM, the selection of optimal collocation points can be challenging and problem-dependent [65]. The method's effectiveness relies on the smoothness of the nonlinear term and its Jacobian. The offline cost for constructing the GNAT basis and points can be substantial [63].

 doi:10.20944/preprints202602.1504.v1

3.2.3. Adaptive Basis Methods

Adaptive basis methods aim to dynamically update or refine the reduced basis during the simulation or parameter exploration to better capture changing solution features, such as moving discontinuities, shocks, or localized phenomena [66,67]. This contrasts with static basis methods like standard POD-Galerkin, where the basis is fixed after the offline stage [67]. Techniques can include incremental POD (iPOD) or local bases defined over subdomains or specific parameter ranges [68].

The workflow often involves an iterative process where the solution is computed, an error indicator is evaluated, and if the error exceeds a threshold, the basis is enriched or adapted [68]. This might mean adding new modes, refining existing ones, or constructing entirely new local bases. For instance, some methods construct adaptive reduced bases using neural networks in the offline stage. The online phase then utilizes this adaptive basis, potentially switching between different local bases or updating the global basis as needed [66].

Adaptive basis methods are particularly effective for problems with complex, evolving dynamics or localized features that are difficult to capture with a single, static global basis [67]. They can significantly improve accuracy for systems where the solution manifold changes drastically [66]. The overhead associated with adaptivity, such as error estimation and basis enrichment, can increase computational cost, sometimes diminishing the benefits of reduction [68]. Designing robust and efficient adaptation strategies and error indicators is a complex task. Managing multiple local bases or dynamically updating a global basis adds complexity to the ROM formulation [66].

3.3. Data-Driven and Machine Learning ROMs

The ROM methodologies discussed in Sections 3.1 and 3.2 are fundamentally physics-intrusive. They require explicit access to and manipulation of the governing equations to construct the ROM through projection or specialized nonlinear approximations. While powerful, this intrusion can be a barrier when high-fidelity simulations are proprietary, overly complex, or when the underlying physics are not fully organized in a tractable PDE form. This limitation has spurred the development of a parallel paradigm: data-driven and machine learning (ML) ROMs. These approaches operate in a non-intrusive manner, treating the high-fidelity model (or experimental system) as a "black box" that generates input-output data. Instead of projecting equations, they employ statistical learning and pattern recognition to construct a direct mapping from system parameters and inputs to the quantities of interest (e.g., temperature fields, phase front location, global heat rate).

3.3.1. Dynamic Mode Decomposition (DMD)

Dynamic Mode Decomposition (DMD) is a data-driven technique that extracts dynamically coherent structures (modes) from time-series data of a dynamical system [69,70]. It approximates the Koopman operator, a linear operator that governs the evolution of observables in a linear fashion, even for nonlinear systems [69,71]. DMD decomposes a sequence of snapshots into a set of modes, each associated with a fixed oscillation frequency and decay/growth rate. This allows for a low-rank, linear representation of potentially nonlinear dynamics [71].

In the offline phase, a sequence of snapshots from the FOM (or experimental data) is collected. DMD then constructs a low-rank linear surrogate model by identifying the dynamic modes and their corresponding eigenvalues that best describe the temporal evolution of the system [69,71]. In the online phase, this linear model is used to predict the future state of the system efficiently, often for various parameter settings, either by propagating the modes or by constructing a reduced-order basis for interpolation [72,73]. Online DMD methods can update the approximation as new data becomes available, making them suitable for streaming datasets [73,74].

DMD is entirely data-driven and "equation-free," requiring no explicit knowledge of the governing equations [71,74]. It provides a linear, interpretable model of complex system dynamics, even for nonlinear systems. Online DMD variants are suitable for real-time applications and streaming data, allowing for dynamic updates to the ROM [73,74]. DMD's performance can be

 doi:10.20944/preprints202602.1504.v1

sensitive to noise in the data and the choice of measurement functions [71]. It often struggles with systems exhibiting strong transient behaviors or highly complex, non-periodic dynamics [75]. The interpretability can diminish for highly complex systems where a large number of modes might be required [69]. When combined with POD and Polynomial Chaos Expansion (PCE), it can construct non-intrusive ROMs for time-dependent stochastic PDEs [76].

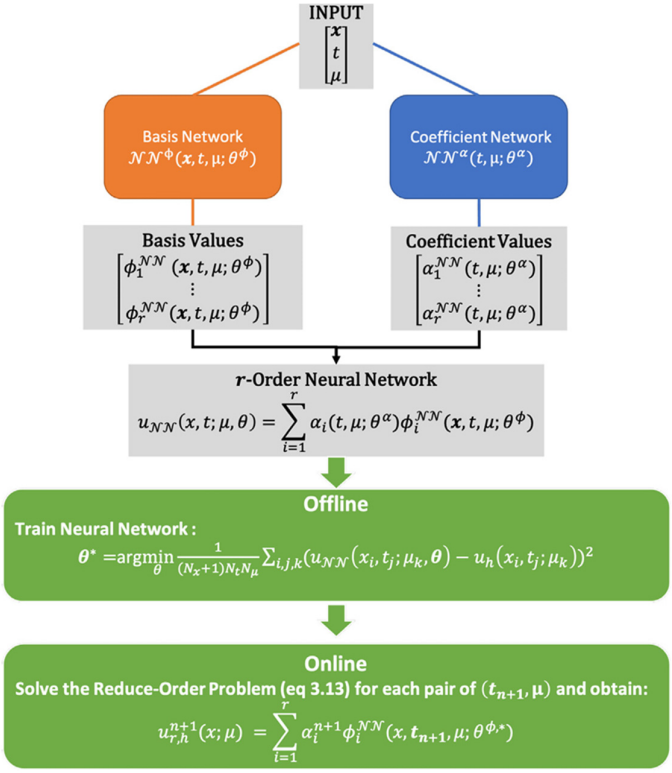

Figure 7. A neural network-based algorithm workflow [66].

3.3.2. Neural Network ROMs

Neural Networks (NNs) offer a powerful way to learn complex, nonlinear mappings between high-dimensional inputs and low-dimensional outputs, or to directly approximate the dynamics of a reduced system [66,70,77]. They can act as surrogate models, learning the input-output relationships of a system, or as components within projection-based ROMs, providing closures or approximating specific nonlinear terms [53]. For instance, a neural network can construct adaptive reduced bases for transport problems [66]. Another application is in physics-informed neural networks (PINNs) where NNs are used within POD-Galerkin ROMs for solving inverse problems [46]. Transformer neural networks can also be used to extract temporal feature relationships from low-dimensional features derived from POD [78].

In the offline phase, a vast amount of high-fidelity data (input parameters, system states, time evolution) is used to train the neural network [66,77]. The NN learns the underlying relationships and builds a compact representation or a predictive model. This training process can be computationally intensive and requires careful hyperparameter tuning [66]. In the online phase, the trained NN quickly predicts system responses for new inputs, offering significant speed-ups compared to FOM simulations [77]. The architecture shown in Figure 7 depicts an overall structure for a neural network-based ROM [66].

NNs are highly flexible and can approximate complex nonlinear relationships effectively, surpassing the limitations of linear ROMs for many challenging problems [70,77]. They are non-intrusive, meaning they do not require direct modification of the FOM code [50,78]. NNs can be used to construct adaptive bases [66] and learn closure terms for projection-based ROMs, improving their

 doi:10.20944/preprints202602.1504.v1

stability and accuracy [53]. Training NNs requires large datasets, which can necessitate extensive FOM simulations in the offline phase [53,77]. They are often considered "black-box" models, lacking the interpretability of physics-based ROMs [70]. Generalization to unseen parameter regimes or extreme conditions can be a challenge, and ensuring physical consistency is an active research area [47].

3.3.3. Autoencoders

Autoencoders are a type of neural network specifically designed for dimensionality reduction [70,79]. They consist of an encoder that maps high-dimensional input data to a low-dimensional latent space (the "bottleneck" layer) and a decoder that reconstructs the original data from this latent representation [80]. By minimizing the reconstruction error, the autoencoder learns an optimal nonlinear manifold embedding, effectively creating a nonlinear reduced basis [70].

In the offline phase, a dataset of FOM snapshots is fed into the autoencoder [80]. The network is trained to compress the data into a low-dimensional latent space and then decompress it back to the original high-dimensional space with minimal loss. This training process captures the essential features of the system's states in the latent variables [79]. In the online phase, new high-dimensional inputs are passed through the trained encoder to quickly obtain their low-dimensional representation in the latent space. Subsequent simulations or analyses can be performed in this reduced space, and the decoder can reconstruct the full-order solution when needed. VpROM, for example, is a variational autoencoder-boosted ROM that defines a generalizable mapping for parametric dependencies in nonlinear systems [80]. Compressed neural networks using pruning and singular value decomposition can further reduce the storage requirements of autoencoders [81].

Autoencoders are powerful for nonlinear dimensionality reduction, capable of discovering optimal nonlinear embeddings for complex data [70,80]. They can capture intricate features that linear methods like POD might miss. The latent space provides a compact and efficient representation of the system state [79]. Similar to other NNs, autoencoders require extensive training data and can be computationally expensive to train [80]. Their black-box nature can hinder physical interpretability and guarantee of physical consistency. The choice of autoencoder architecture and hyperparameters significantly impacts performance [79]. Compared to POD and DMD, autoencoders can have larger storage requirements, though compression techniques exist to mitigate this [81].

3.3.4. Gaussian Process ROMs

Gaussian Process (GP) models are non-parametric, Bayesian approaches to regression and function approximation. When applied to ROMs, GPs can model the relationship between system parameters and reduced-order coefficients or directly approximate the system's response in the reduced space. They provide not only predictions but also a measure of uncertainty (variance) associated with those predictions, which is a key advantage [70].

In the offline phase, a sparse set of FOM solutions (snapshots) for various parameter values is used to train the GP model. The GP learns the mapping from parameters to the reduced solution space, typically involving the definition of a covariance function (kernel) that encodes assumptions about the smoothness and correlation of the function being approximated. In the online phase, for new parameter inputs, the trained GP can rapidly predict the corresponding reduced-order solution, along with an associated uncertainty quantification, without requiring additional FOM evaluations [70].

GPs provide inherent uncertainty quantification, which is crucial for applications like robust design and risk assessment. They are highly flexible and can model complex, nonlinear relationships with relatively small datasets compared to deep neural networks [70]. GPs can be particularly effective for exploring parameter spaces where FOM evaluations are costly. The computational cost of GP inference scales cubically with the number of training data points, limiting their applicability to very large datasets. Choosing an appropriate kernel function is critical for performance and can be

 doi:10.20944/preprints202602.1504.v1

problem-dependent. They can sometimes struggle with very high-dimensional parameter spaces or problems with sharp discontinuities in the solution manifold [70].

3.4. Comparative Summary of Common ROM Methodologies

The spectrum of ROM techniques detailed in Sections 3.1 to 3.3 represents a continuum from rigorous, physics-intrusive projection methods to flexible, equation-free data-driven surrogates. Each category offers a distinct balance between fidelity to first principles, computational efficiency, and implementation complexity, making them differentially suited to specific stages of the LHS system lifecycle—from initial design exploration to real-time control and digital twinning.

Table 1. Summary of common ROM methodologies.

Characteristic	Projection-Based Linear ROMs	Nonlinear & Hyper-Reduced ROMs	Data-Driven & ML ROMs
Core Philosophy	Project governing equations onto a low-dimensional linear subspace.	Extend projection methods to handle nonlinearity via term approximation or basis adaptation.	Learn system behavior directly from data, bypassing explicit equation reduction.
Intrusiveness	Intrusive: Requires full access to and manipulation of FOM equations.	Intrusive: Requires access to FOM equations and nonlinear terms.	Non-Intrusive: Treats FOM as a black-box data generator.
Handling of PCM Nonlinearity	Poor. Linear subspaces struggle with moving boundaries and enthalpy jumps. Often requires many modes.	Good to Excellent. DEIM/GNAT approximate nonlinear terms; adaptive bases track evolving dynamics.	Excellent. ML models (NNs, GPs) are inherently flexible nonlinear function approximators.
Offline Cost & Complexity	High. Requires FOM snapshot generation and matrix decompositions (e.g., SVD).	Very High. Adds complex steps: nonlinear term snapshot generation, magic point selection, or basis adaptation logic.	Highest. Demands extensive FOM runs for training data and computationally intensive model training/tuning.
Online (Runtime) Performance	Very Fast. Solving a small ODE system.	Fast. Solving a small ODE system with pre-computed sparse evaluations.	Extremely Fast. Typically a simple forward pass through a trained model (e.g., NN).
Interpretability & Physical Consistency	High. Structure mirrors original physics; Galerkin projection ensures certain conservation properties.	Moderate to High. Physics-based core remains, but approximations reduce strict consistency.	Low ("Black-Box"). Internal logic is opaque; predictions may violate physical laws without constraints (e.g., PINNs).
Generalizability & Extrapolation	Moderate. Limited to parameter/state space	Moderate. Similar to linear ROMs, but adaptive	Poor. Performance degrades rapidly

 doi:10.20944/preprints202602.1504.v1

	sampled for basis generation.	methods can improve within bounds.	outside the convex hull of the training data.
Best-Suited Applications	Linear subsystems, sensitivity analysis, problems with strong coherent structures.	High-fidelity control, digital twins where nonlinear physics must be retained with some efficiency.	Rapid design optimization, system-level simulation, complex geometries where intrusive reduction is infeasible.
Key Enabling Technology for PCM-based LHS	POD-Galerkin for conduction-dominated regimes; RB for parametric studies.	DEIM/GNAT for enthalpy-porosity models; adaptive bases for tracking phase fronts.	ANN/XGBoost surrogates for complex finned/triplex-tube systems; autoencoders for nonlinear field compression.

Projection-Based Linear ROMs are the most interpretable and mathematically founded. They excel in systems where the dynamics are dominated by coherent structures that can be captured in a low-rank linear subspace. Their key strength lies in preserving a direct, albeit reduced, connection to the original governing equations, which aids in understanding and trust. However, their fundamental assumption of linearity is their primary weakness when applied to the strongly nonlinear, moving-boundary problems inherent in PCM phase change. While they can achieve significant speed-ups for linear or weakly nonlinear components, they often become inefficient or inaccurate for full charging/discharging cycles without augmentation.

Nonlinear and Hyper-Reduced ROMs evolved directly to address the core limitation of projection-based linear ROMs methods: handling system nonlinearity while maintaining an intrusive, physics-based structure. Techniques like DEIM and GNAT preserve the projection framework but introduce sophisticated approximations (e.g., sparse sampling of nonlinear terms) to recover computational efficiency. Adaptive basis methods further enhance flexibility by allowing the reduced subspace to evolve with the solution. These methods represent a powerful compromise, offering improved nonlinear capability while retaining more interpretability than purely data-driven models. Their trade-off is increased algorithmic and implementation complexity in the offline stage.

Data-Driven and Machine Learning ROMs represent a paradigm shift. They forgo the explicit projection of equations in favor of learning input-output relationships or low-dimensional embeddings directly from data. This non-intrusive nature is their greatest asset, allowing for integration with complex or proprietary FOMs and providing extreme flexibility in modeling nonlinear and even non-physical correlations. They have demonstrated remarkable speed-ups for complex geometries (e.g., finned enclosures). Their principal liabilities are the "black-box" nature, which complicates physical interpretation and validation; a high demand for comprehensive, high-quality training data; and a general lack of built-in guarantees for physical consistency or extrapolation robustness.

The choice among these methods is not a question of which is universally superior, but which is most fit-for-purpose given the application's requirements for accuracy, speed, interpretability, and available resources (data, FOM access, expertise). Table 1 provides a concise comparison of the three primary ROM categories across key attributes relevant to PCM-based LHS system modeling. With this methodological foundation established, Section 4 examines why these ROM techniques are particularly valuable—and challenging—for PCM-based LHS applications.

4. Applicability of ROMs to PCM-Based Latent Heat Storage Systems

ROMs are essential for efficiently simulating complex thermal systems, particularly in the context of PCM-based latent heat storage systems [2,9,82]. These systems exhibit high energy density

 doi:10.20944/preprints202602.1504.v1

and isothermal storage capabilities, making them attractive for various applications, including solar engineering, building heating and cooling, and thermal management of electronic devices [23,83–85]. However, the detailed simulation of PCM systems, which involves phase change, conduction, and convection, can be computationally intensive, necessitating the use of ROMs to reduce computational cost while maintaining sufficient accuracy [9,33,86]. ROMs are particularly applicable to PCM-based LHS systems because they can capture the dominant thermal dynamics without the need for detailed spatial discretization at every time step [87,88].

4.1. Advantages of ROMs in Latent Heat Storage Systems

ROMs enable faster iteration cycles during the design phase of PCM-based TES systems. Engineers can quickly evaluate different PCM types, encapsulation methods, or heat exchanger geometries to optimize performance. For instance, a ROM of encapsulated PCMs can be used to study the effects of porosity, capsule diameter, and heat transfer fluid (HTF) flow rate on overall system performance [82]. Studies have developed approximation-assisted reduced-order PCM heat exchanger models to speed up the design process of thermal energy storage devices [1].

For effective operation and control of LHS systems, particularly in applications like building-integrated TES, real-time feedback is crucial [89,90]. ROMs can provide rapid predictions of the system's thermal state, enabling proactive control strategies for charging and discharging cycles [91]. This is vital for managing the intermittent nature of renewable energy sources, such as solar or wind power, by balancing energy supply and demand.

Predicting the thermal response of a PCM system and estimating its state-of-charge (SOC) is challenging due to the nonlinearity introduced by phase change [86]. ROMs, especially those validated against experimental data, can accurately predict transient thermal output and SOC, crucial for efficient energy management (Ezzat Khalifa & Koz, 2018). A 1D ROM, for example, has been developed for a novel latent thermal energy storage system addressing challenges like low thermal conductivity and expensive encapsulation processes [2].

PCMs often suffer from low thermal conductivity and potential leakage during phase transitions. Strategies to mitigate these issues include microencapsulation or the addition of highly conductive filler materials [93–95]. ROMs can effectively model the enhanced heat transfer in these composite materials. Different types of PCMs, including organic (e.g., paraffin), inorganic (e.g., salt hydrates), and eutectic mixtures, have varying thermal properties and operating temperature ranges. These can be categorized by their melting temperatures, from low-temperature PCMs like ice and water gel to high-temperature PCMs such as molten salts and metal alloys [96]. The selection of appropriate PCM depends on the application, ranging from transient thermal management of electronic devices, where rapid heat absorption is needed, to seasonal thermal energy storage (STES) for long-term energy balancing [97,98]. ROMs can aid in understanding how different PCM characteristics influence overall system performance across these diverse applications.

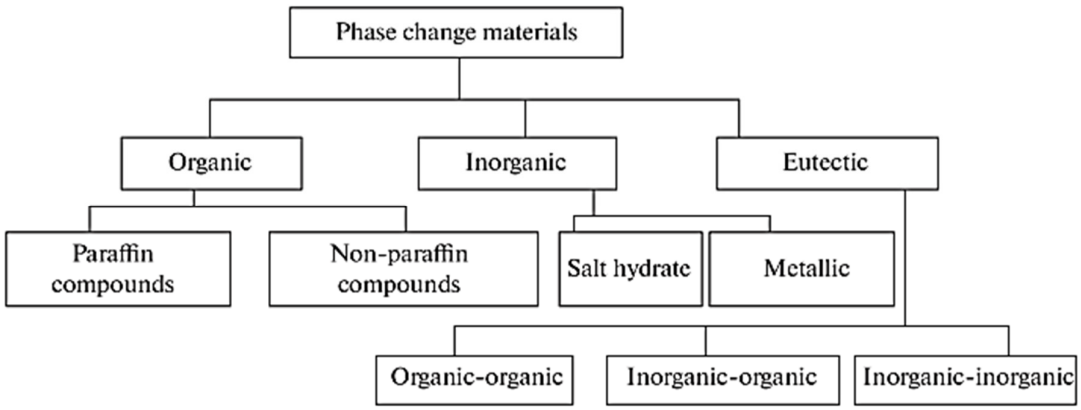

Figure 8. Classifications of PCM based on its content [96].

 doi:10.20944/preprints202602.1504.v1

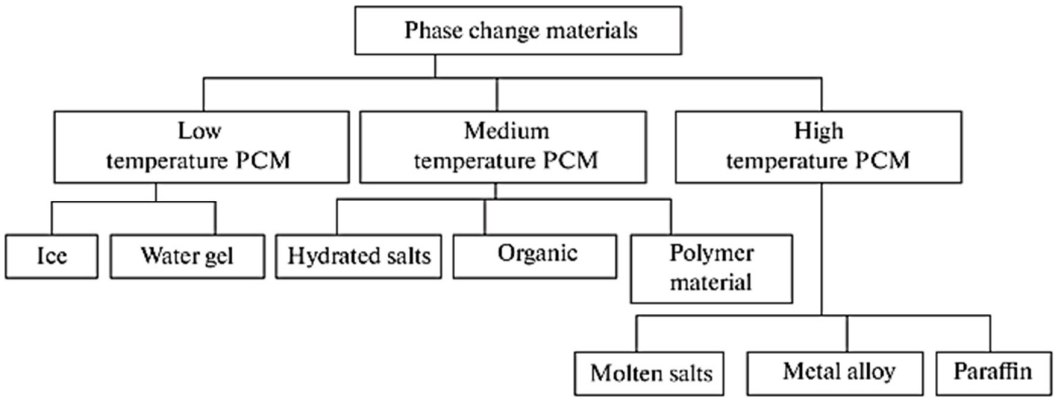

Figure 9. Classification of PCM based on melting temperature [96].

4.2. Core Challenges in PCM-Based LHS Modeling

While ROMs offer significant benefits, their development and deployment in PCM-based latent heat storage (LHS) systems are accompanied by notable challenges. It is complicated by four interconnected physical phenomena, each introducing distinct modeling difficulties. [99,100].

4.2.1. Latent Heat Nonlinearity

The dominant source of nonlinearity originates from the phase change process itself [101–103]. During melting and solidification, PCMs exhibit highly nonlinear thermophysical behavior: the enthalpy-temperature relationship becomes strongly nonlinear in the phase transition region, and key properties—specific heat, thermal conductivity, density—vary substantially between solid and liquid phases [104]. This nonlinearity is compounded by buoyancy-driven natural convection in the molten phase, which creates spatially nonuniform temperature and velocity fields that depend on local thermal gradients and geometry [105,106]. Hysteresis between melting and solidification further complicates prediction, as the material's thermal history influences its response [99]. Together, these nonlinear effects mean that linear modeling approaches fundamentally cannot capture PCM dynamics, necessitating either nonlinear projection methods (Section 3.2) or flexible data-driven surrogates (Section 3.3).

4.2.2. Moving Phase Boundaries

The solid-liquid interface propagates dynamically through the material, forming a boundary that is inherently time-dependent and unknown a priori [107–109]. This moving boundary problem—classically known as the Stefan problem—requires simultaneous solution for temperature fields and interface position [110]. Fixed-grid methods like enthalpy-porosity avoid explicit interface tracking but introduce numerical challenges: fine spatial discretization is needed to resolve the phase front, and non-physical behavior can arise in close-contact melting scenarios where velocity errors exceed 50% [111]. Density changes between phases cause volumetric expansion or contraction as the interface advances, further complicating energy balances [112]. From a ROM perspective, moving boundaries mean that the solution's dominant spatial features evolve, challenging static basis assumptions and motivating adaptive methods (Section 3.2.3).

4.2.3. Multi-Timescale Dynamics

PCM systems inherently exhibit dynamics spanning multiple timescales [113]. Latent heat absorption or release occurs rapidly over short intervals, while conduction in solid phases and convection in liquid phases evolve more gradually. Cascaded latent heat storage systems compound this complexity, as individual PCM layers may undergo phase change asynchronously [114]. The dynamic response can span from sub-millisecond thermal transients to charging/discharging processes lasting hours [115]. This wide range challenges variable time-step solvers, which often

 doi:10.20944/preprints202602.1504.v1

encounter convergence difficulties during rapid phase change events [116]. For ROMs, multi-timescale behavior demands that reduced bases capture both fast and slow modes; projection-based methods may require many modes to represent the full temporal spectrum, while data-driven methods need training data that adequately samples all relevant timescales.

4.2.4. Geometry and Boundary Sensitivity

Performance is strongly influenced by both geometric configuration and imposed boundary conditions [117–119]. The shape, orientation, and aspect ratio of the PCM enclosure affect heat transfer pathways, natural convection development, and phase change uniformity [120,121]. Enhancement techniques—fins, metal foams, encapsulation—further increase geometric complexity and parameter sensitivity [101,122,123]. Boundary conditions (constant temperature, constant heat flux, cyclic operation) directly determine charging/discharging behavior and must be accurately represented in ROMs [124,125]. This sensitivity means that ROMs trained for one configuration rarely generalize to others; each geometry or boundary condition change typically requires new training data or basis construction, limiting transferability.

The advantages and challenges discussed above are concretely illustrated in the following case studies, which demonstrate how different ROMs perform across diverse LHS configurations.

5. ROMs for PCM-Based Latent Heat Storage Systems

The development of ROMs for LHS systems has evolved along several methodological trajectories, each balancing computational efficiency against physical fidelity. Current approaches range from physics-based analytical models to data-driven machine learning techniques, with hybrid methods combining the strengths of both paradigms [9]. This section examines studies representing the state-of-the-art in ROM development for LHS systems, reporting their LHS configuration and physical scope, governing physics incorporated into the ROM, the chosen ROM methodology and model class, snapshot or training strategy, model order and associated computational cost, accuracy metrics and validation approach, intended application and use case, as well as reported limitations.

5.1. Two-Temperature Non-Equilibrium ROM for Packed Bed Systems

A reduced-order model was developed for LHS systems consisting of spherical capsules filled with PCM, arranged in a packed bed configuration [82]. The physical domain used in the study consists of a cylindrical storage tank (460 mm length × 360 mm diameter) containing eight layers of evenly packed spherical capsules, as shown in Figure 10, with 55 mm inner diameter and 0.8 mm wall thickness. The system uses paraffin as the PCM with a melting temperature of 333 K, while water serves as the heat transfer fluid (HTF) flowing through the interstitial spaces between capsules. The model addresses the charging process where hot HTF melts the encapsulated PCM, with porosity of 0.451 representing the volume fraction available for fluid flow. The ROM reduces the entire three-dimensional packed bed to a one-dimensional formulation along the flow direction, treating the system as a porous medium with distributed thermal capacitance. This dimensional reduction is justified by assuming negligible temperature gradients in the radial direction and uniform behavior within each horizontal layer of capsules. The model scope encompasses parametric variations in porosity, capsule diameter, capsule shell thickness, and HTF mass flow rate to assess their influence on thermal performance during charging.

 doi:10.20944/preprints202602.1504.v1

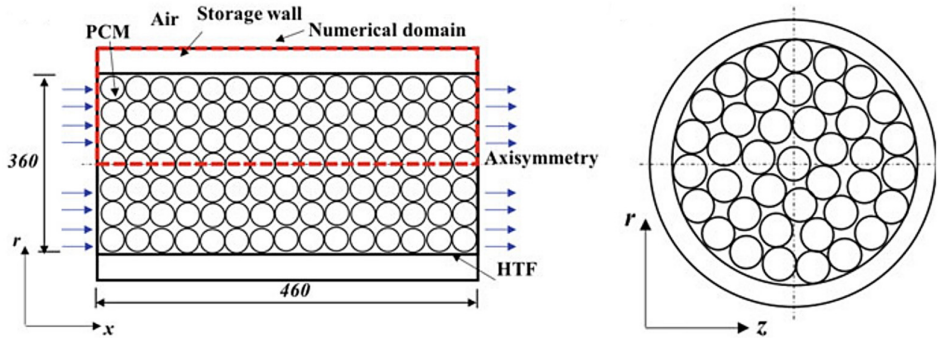

Figure 10. Physical domain of the LHS with spherically encapsulated PCM [82].

The governing physics are captured through a two-temperature non-equilibrium energy equation framework, where separate energy balances are formulated for the HTF and PCM phases. This approach recognizes that thermal equilibrium between the fluid and solid phases is not instantaneously achieved, with heat transfer resistance governing the temperature difference between phases. The HTF energy equation accounts for convective transport along the flow direction and interfacial heat exchange with the PCM capsules, while the PCM energy equation incorporates the enthalpy method to handle phase change. The enthalpy method treats the phase transition by defining total enthalpy as the sum of sensible and latent components, with the liquid fraction serving as the phase indicator. This formulation eliminates explicit interface tracking while naturally accommodating the phase change over a temperature range. The interfacial heat transfer between HTF and PCM is modeled using empirical correlations for flow over spheres, with the Nusselt number depending on Reynolds and Prandtl numbers. Heat losses to the ambient environment are incorporated through a thermal resistance boundary condition on the tank wall. Notably, the model neglects convection within the liquid PCM contained in each capsule, treating heat transfer within the capsule as purely diffusive. This assumption is justified for small-diameter capsules where conduction dominates but may introduce errors for larger capsules where natural convection becomes significant. The model also assumes isothermal phase change and neglects PCM expansion/contraction during melting.

The ROM employs finite volume discretization along the axial direction, dividing the storage length into discrete control volumes. Each control volume contains both HTF and PCM, with their energy equations solved simultaneously. The model uses only five grid points in the axial direction, representing a drastic reduction from the thousands of cells required in a three-dimensional CFD simulation. This coarse discretization is enabled by the one-dimensional assumption and the use of lumped heat transfer coefficients to represent interfacial phenomena. The numerical solution proceeds using an implicit time-stepping scheme, solving the coupled algebraic equations for HTF and PCM temperatures at each time level. The phase change is handled through an iterative update of the liquid fraction based on the local enthalpy and temperature. Pressure drop across the storage is calculated using empirical correlations for flow through packed beds, accounting for both viscous and inertial losses. The ROM was implemented in MATLAB, with computational efficiency being a primary advantage. While exact timing comparisons with full-order models are not provided in the paper, the five-point spatial discretization and implicit time integration enable rapid simulation of charging processes that would require substantially more computational effort with detailed CFD. The sequence of steps followed in developing this ROM—from physical simplifications to numerical implementation and solution strategy—is summarized in Figure 11.

 doi:10.20944/preprints202602.1504.v1

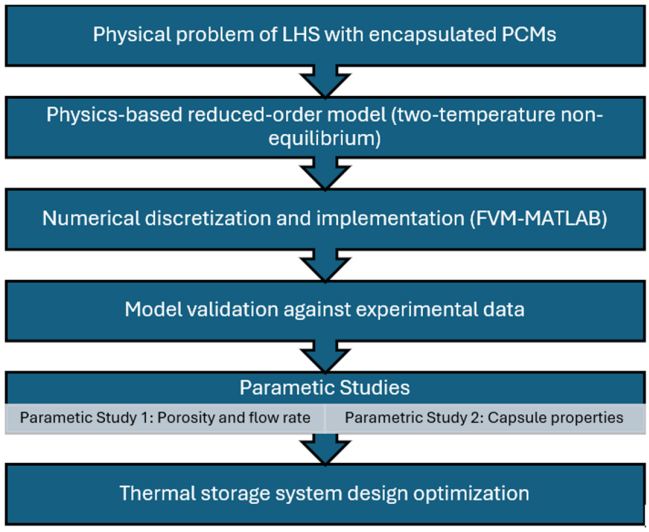

Figure 11. Reduced-order modeling workflow for the two-temperature packed-bed PCM-based LHS system [82].

The ROM validation relied on experimental data from published literature rather than generating a dedicated training dataset. The validation case used a storage system with identical geometry to the experimental setup, matching the HTF inlet temperature (343 K), flow rate (2 L/min), and initial PCM temperature (305 K). The heat transfer coefficient on the outer tank wall was calibrated to 2.92 W/m²·K based on ambient conditions. The comparison between predicted and measured HTF outlet temperatures showed maximum deviations of 2.5 K throughout the charging process. The model successfully captured the thermal stabilization period when the PCM reaches its melting temperature, as well as the subsequent temperature rise after complete melting. The close agreement validated both the two-temperature framework and the enthalpy method implementation. Following validation, parametric studies explored the effects of porosity (varying capsule packing density), capsule diameter, shell thickness, and HTF mass flow rate on system performance. These studies revealed that stabilization time—the period during which PCM actively absorbs latent heat—increases with low porosity and low mass flow rate, while capsule shell thickness has negligible influence on heat transfer.

The model order is characterized by five spatial grid points along the axial direction, with two dependent variables (HTF and PCM temperatures) at each point. This results in approximately 10 primary state variables, plus additional variables for tracking liquid fraction and other quantities. This represents a reduction of several orders of magnitude compared to full three-dimensional CFD models that would require millions of degrees of freedom to resolve the interstitial flow and individual capsule heat transfer. The computational cost of the ROM is not explicitly quantified in terms of wall-clock time or speed-up factors. However, the use of five grid points and implicit time integration suggests simulation times on the order of seconds to minutes for typical charging scenarios. This enables rapid parametric studies and design optimization that would be prohibitive with high-fidelity models.

The primary accuracy metric is the maximum temperature deviation between predicted and measured HTF outlet temperatures, which remained below 2.5 K across the entire charging process. This corresponds to a relative error of approximately 0.7% based on the temperature difference between inlet HTF and initial PCM temperature. The model's main limitations stem from its fundamental assumptions. The neglect of natural convection in liquid PCM may underpredict heat transfer rates for larger capsules or high-viscosity PCMs where convection becomes significant. The one-dimensional assumption breaks down for storage systems with large diameter-to-length ratios or non-uniform flow distribution. The model also requires empirical heat transfer correlations that

 doi:10.20944/preprints202602.1504.v1

may not be accurate outside their calibration range, and it cannot predict detailed flow patterns or local hot spots that might be important for certain applications.

The intended application is solar thermal storage systems where packed-bed LHS units store excess thermal energy during periods of high solar irradiation for later use. The ROM enables rapid assessment of how design parameters (porosity, capsule size) and operating conditions (flow rate, inlet temperature) affect storage capacity, charging time, and thermal efficiency. This supports optimization of storage system design for specific solar thermal installations. The model is particularly suited for system-level simulations where the LHS unit is coupled with solar collectors, heat exchangers, and thermal loads. The computational efficiency allows the storage model to be embedded in larger energy system models without becoming a bottleneck. Potential extensions could include discharging process simulation and integration with controls for optimal charge/discharge scheduling.

5.2. Approximation-Assisted ROMs for PCM Heat Exchangers

A two complementary reduced-order modeling approaches (i.e., black-box and grey-box model) for PCM-embedded heat exchangers were developed and used in thermal energy storage applications [1]. The physical system consists of n-tetradecane PCM embedded in a thermally conductive graphite matrix, forming a composite that enhances the effective thermal conductivity while maintaining high latent heat capacity. The PCM-graphite composite is integrated into a heat exchanger geometry where heat transfer fluid flows through channels, exchanging thermal energy with the PCM. The ROM development targets rapid prediction of PCM HX performance across a wide design and operating space. The design variables include PCM transition temperature, fluid mass flow rate, and PCM slab thickness, defining a three-dimensional parameter space that must be explored during optimization. The inlet fluid conditions (temperature and mass flow rate) vary dynamically during charging and discharging, requiring the ROM to accurately predict transient thermal behavior under time-varying boundary conditions.

Unlike physics-derived reduced models, this approach follows a CFD-informed ROM development strategy in which high-fidelity simulations serve as a data generator for constructing a fast predictive surrogate. The overall process does not reduce the governing equations directly, but instead transforms CFD outputs into an efficient reduced representation through data extraction, training, and validation stages. The overall workflow by which finite-volume simulation data are transformed into black-box and grey-box reduced-order representations is illustrated in Figure 12.

 doi:10.20944/preprints202602.1504.v1

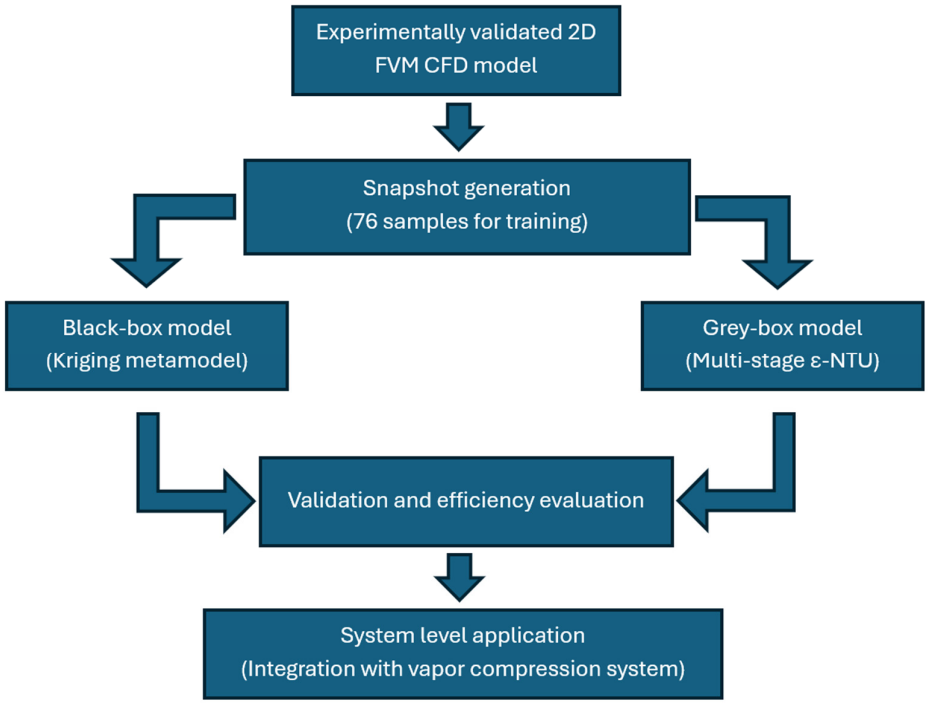

Figure 12. ROM development workflow for CFD-informed ROMs for PCM-embedded heat exchangers [1].

Two distinct ROM formulations were developed: a pure black-box model and a physics-informed grey-box model. The black-box model treats the PCM HX as an input-output system without explicit representation of internal physics, relying entirely on data-driven correlations. In contrast, the grey-box model incorporates simplified heat transfer physics through the effectiveness-NTU (ε-NTU) method, which provides an analytical framework for heat exchanger performance. The ε-NTU method in the grey-box model represents the PCM using a two-node thermal network: one node for solid PCM at the transition temperature and one for sensible heat storage in liquid or solid regions. The effectiveness parameter characterizes the heat exchanger's ability to transfer heat between the fluid and PCM, while the Number of Transfer Units quantifies the ratio of thermal capacitance to heat transfer resistance. This formulation captures the essential physics of heat exchange and phase transition while maintaining computational simplicity. Neither model explicitly resolves spatial temperature distributions within the PCM or detailed flow patterns in the fluid channels. Heat transfer is instead characterized through lumped parameters (effectiveness, NTU) or direct metamodel predictions (black-box). This level of abstraction enables rapid evaluation but sacrifices detailed local information about phase front progression or temperature gradients.

The black-box model employs Kriging metamodeling, a Gaussian process regression technique that interpolates function values based on spatial correlation structures. Training data consisting of input parameters (fluid inlet temperature difference from PCM transition temperature, mass flow rate, PCM thickness) and output responses (PCM HX heat rate as a function of time) are generated using a validated finite-volume model. The Kriging metamodel learns the complex nonlinear mapping from inputs to transient heat rate trajectories, enabling rapid prediction for new parameter combinations not explicitly simulated during training. The grey-box model structure divides the transient thermal response into distinct periods based on the dominant heat transfer mechanism. During the primary phase change period, the ε-NTU method predicts heat transfer with the PCM maintained at its transition temperature. After phase change completion, a second period models sensible heating or cooling of fully solid or liquid PCM. Time periods demarcating these transitions are predicted using metamodel correlations trained on finite-volume simulation results. Both models operate without spatial discretization of the PCM domain, instead predicting global quantities like total heat transfer rate and outlet fluid temperature. This lumped-parameter approach enables time

 doi:10.20944/preprints202602.1504.v1

steps of 1 second compared to the millisecond-scale steps required for explicit finite-volume schemes, contributing significantly to computational acceleration.

The training dataset was generated using a validated two-dimensional finite-volume model that resolves conduction in the PCM-graphite composite and convection in the fluid channels. The sampling strategy employed Latin Hypercube Sampling to efficiently cover the three-dimensional design space with 38 sample points per design space (melting and solidification considered separately). This structured sampling ensures good space-filling properties and captures the design space more efficiently than random sampling. Eight corner points were added to the LHS samples to ensure the design space boundaries are adequately represented. The total training library thus consisted of 76 high-fidelity simulations (38 samples × 2 design spaces), with each simulation requiring 13 to 127 seconds depending on the melting/solidification time. For the black-box model, the training data consists of time series of heat rate for each sample point, while the grey-box model extracts characteristic time periods and effectiveness values from the same simulations. The finite-volume training simulations used an explicit time-stepping scheme with fine spatial resolution to ensure accuracy. The computational investment in training data generation is substantial (approximately 1-2 hours total), but this one-time cost enables unlimited rapid predictions across the entire design space.

The model order differs fundamentally between the two approaches. The black-box Kriging metamodel has no explicit state variables, instead directly predicting output quantities from input parameters through learned correlation functions. The effective dimensionality is determined by the number of training samples that define the Gaussian process. The grey-box model has approximately 2-3 state variables representing PCM node temperatures and phase state, making it slightly more complex but still drastically simplified compared to the baseline finite-volume model with thousands of degrees of freedom. Computational performance comparisons against the finite-volume baseline revealed dramatic speed-ups, as shown in Figure 13. The finite-volume model required an average of 44 seconds per verification case, while the grey-box model completed the same simulation in 2.5 seconds and the black-box model in 0.2 seconds. This yields speed-up factors of approximately 18× for the grey-box model and 220× for the black-box model on a component level. When integrated into a complete vapor compression system for thermal energy storage, the system simulation time decreased from an average of 1465 seconds using the finite-volume PCM HX model to 59 seconds using the reduced-order models. This represents a speed-up of 25-57× at the system level, enabling design optimization and control studies that would be computationally prohibitive with high-fidelity models.

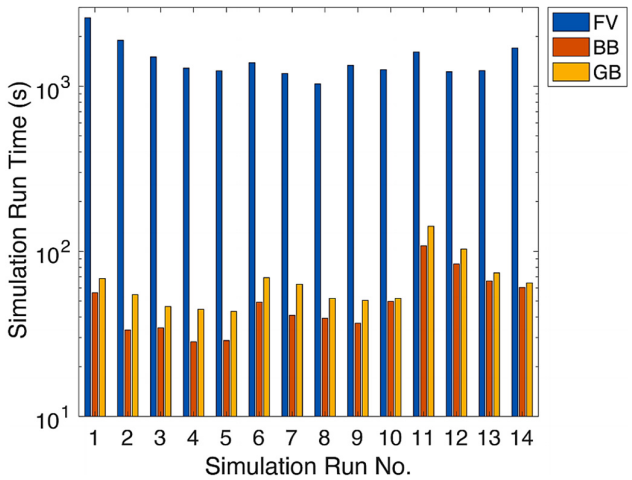

Figure 13. Computational cost reduction of black-box and grey-box models from finite volume model [1].

 doi:10.20944/preprints202602.1504.v1

Model accuracy was assessed using 1000 verification points (500 for melting, 500 for solidification) randomly sampled from the design space. The black-box model achieved a mean absolute error in fluid outlet temperature of 0.05 K, while the grey-box model had a slightly higher error of 0.10 K. Maximum errors reached 0.31 K and 0.50 K for the black-box and grey-box models respectively during melting processes. The grey-box model showed larger temperature deviations toward the end of the phase change process due to its simplified two-node PCM representation. The assumption of instantaneous transition between phase change and sensible heat periods introduces discontinuities not present in the actual physical system, leading to localized prediction errors. The black-box model, unconstrained by this structural simplification, achieved better accuracy through its more flexible functional form. At the system level, when integrated with a vapor compression system, the mean absolute deviation in compressor energy consumption was 0.2% for the black-box model and 0.3% for the grey-box model. Total charging time predictions showed deviations of 1.1% and 2.6% respectively. These remarkably low system-level errors demonstrate that local temperature prediction errors do not necessarily propagate to integral performance metrics due to compensating effects.

The primary application is accelerated design and optimization of PCM-based thermal energy storage devices for building HVAC systems and renewable energy integration. The ROMs enable rapid evaluation of hundreds or thousands of design alternatives to identify optimal PCM selection, heat exchanger geometry, and operating strategies. The computational efficiency particularly benefits multi-objective optimization problems where Pareto frontiers must be mapped across competing objectives like capital cost, storage capacity, and round-trip efficiency. The models are also suited for system-level simulation where the PCM HX couples with vapor compression cycles, solar collectors, or building thermal loads. The near-instantaneous evaluation enables day-long or season-long simulations with hourly or sub-hourly time resolution, supporting analysis of energy cost savings, peak demand reduction, and grid interaction strategies.

Several limitations constrain the applicability of these ROMs. Both models assume one-dimensional heat transfer perpendicular to the flow direction, neglecting multi-dimensional effects that may be important for complex geometries. Natural convection within liquid PCM is not explicitly modeled, though its effects may be implicitly captured in the training data. The models do not account for PCM degradation, subcooling, or hysteresis effects that can occur in real systems after many thermal cycles. The black-box model requires substantial training data covering the entire operating range of interest, and extrapolation beyond the training domain can produce unreliable predictions. The grey-box model's two-node PCM representation limits accuracy during transition periods between phase change and sensible heat modes. Neither approach provides detailed information about local temperature distributions or phase front locations, which may be important for identifying hot spots or optimizing internal heat transfer enhancement features.

5.3. POD-Based ROM for Direct Steam Generation Solar Thermal Power

Researchers developed a Proper Orthogonal Decomposition (POD) reduced-order model specifically targeting latent heat storage processes in direct steam generation solar thermal power (DSG-STP) systems [8]. The physical configuration consists of a shell-and-tube heat exchanger where saturated steam at 10.7 bar flows through tubes while PCM undergoes phase change in the shell side. This high-temperature application (steam temperatures near 180°C) presents unique challenges compared to lower-temperature building applications, including both vapor-liquid phase change in the HTF and solid-liquid phase change in the PCM. The ROM addresses unsteady-state heat transfer with simultaneous phase change occurring in both the PCM and the steam/water HTF. The system geometry includes internal tube arrays surrounded by PCM, with specific attention to modeling the vapor-liquid interface movement in the HTF tubes and the solid-liquid interface in the PCM region. The model scope encompasses variations in steam inlet conditions and time-dependent boundary conditions representative of solar thermal plant operation where steam generation rates fluctuate with solar irradiance.

 doi:10.20944/preprints202602.1504.v1

The full-order model underlying the POD-ROM combines the Lee model for vapor-liquid phase change with the enthalpy-porosity approach for PCM melting. The Lee model governs condensation and evaporation of the steam/water HTF by introducing source terms in the mass and energy equations based on the local temperature relative to the saturation temperature. The vapor mass fraction serves as the primary indicator of the phase state in the HTF domain. For PCM phase change, the enthalpy-porosity method treats the mushy zone as a porous medium with porosity equal to the liquid fraction. As the PCM melts, the liquid fraction evolves from zero (fully solid) to one (fully liquid), with momentum equations including a Darcy-type source term that suppresses velocity in the solid regions. This formulation naturally handles the moving solid-liquid interface without explicit tracking. The coupling between HTF and PCM occurs through conjugate heat transfer boundary conditions at the tube walls. The full-order model solves the complete set of conservation equations (mass, momentum, energy) in both domains using finite volume methods. Natural convection in liquid PCM is captured through the Boussinesq approximation, accounting for density-driven flow that can significantly enhance heat transfer compared to pure conduction.

The POD approach extracts dominant spatial patterns (modes) from an ensemble of full-order solution snapshots through singular value decomposition (SVD). Snapshots representing the temperature field at different time instants are arranged as columns in a matrix, and SVD identifies the orthogonal basis functions that optimally represent the ensemble in a least-squares sense. The energy contribution of each mode quantifies how much of the total variance it captures, allowing selection of the minimum number of modes needed to achieve a target accuracy. For the DSG-STP application, the temperature field is decomposed as a linear combination of POD basis functions with time-varying coefficients. The key reduction comes from retaining only the most energetic modes (typically 1-5) while discarding higher-order modes that contribute little to the overall variance. This compression from potentially millions of spatial degrees of freedom to a handful of coefficients enables dramatic computational savings. The POD coefficients (time-varying amplitudes of each mode) are obtained through interpolation methods rather than solving reduced-order differential equations. Snapshots at a limited number of time instants and operating conditions are generated using the full-order model, POD modes are extracted, and the coefficients for new conditions are interpolated from the snapshot database. This non-intrusive approach avoids the complexity of Galerkin projection and makes the ROM easy to implement. The sequence of steps followed in constructing this POD-based ROM is summarized in Figure 14.

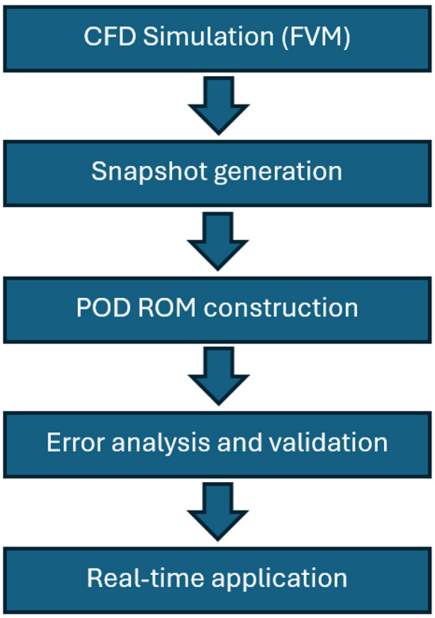

Figure 14. ROM development of POD-based ROM for DSG-STP system [8].

 doi:10.20944/preprints202602.1504.v1

Training data consisted of 13 optimal trajectories generated by solving the full-order model with the Lee model and enthalpy-porosity approach. Each trajectory was sampled at 10 uniformly distributed time steps over a 0.5-second simulation window (with 0.05-second intervals), yielding 130 total snapshots. The operating parameters varied included the angle of attack (sampled in the range of -1.0 to 1.0 radians) and time, creating a two-dimensional parameter space. The full-order simulations required substantial computational effort, with each trajectory taking approximately 20 minutes on a single CPU core. This investment in generating high-quality training data is essential for POD-ROM accuracy, as the basis functions must adequately span the solution manifold across the operating range of interest. After extracting POD modes from the training snapshots, the modes are used to compress and reconstruct test data not included in the training set. The reconstruction error—the difference between the full-order snapshot and its POD approximation—provides a measure of how well the modes capture the essential dynamics. Acceptable reconstruction errors indicate that the POD basis is sufficiently rich.

The model order is characterized by the number of POD modes retained, which varied from 1 to 5 depending on the field variable and desired accuracy. For temperature predictions, using 5 POD modes achieved accumulative energy contributions exceeding 99%, meaning the retained modes capture 99% of the variance in the training data. Velocity and vapor mass fraction fields required similar mode counts. The computational speed-up achieved by the POD-ROM is substantial. For one test case (Case A), the finite volume method required approximately 4 hours of simulation time, while the POD model completed the same simulation in 45.865 seconds. This represents a speed-up factor of approximately 314×, reducing a prohibitively expensive simulation to near-interactive speeds. The speed-up stems from multiple sources: elimination of spatial discretization (replaced by mode amplitudes), larger allowable time steps in the coefficient interpolation, and avoidance of iterative solution of nonlinear equations at each time step. The POD prediction simply evaluates a linear combination of pre-computed basis functions, requiring minimal computational effort.

Accuracy was quantified using relative mean error (RME) comparing POD predictions to full-order finite volume results. For temperature fields, the RME remained below 0.1% across all test cases, demonstrating excellent agreement. This remarkably low error reflects both the effectiveness of POD for smooth thermal fields and the adequate sampling of the parameter space during training. For vapor mass fraction—a more challenging quantity due to its discontinuous nature across phase boundaries—the POD-ROM also showed good performance when using 5 basis functions. The accumulative energy contribution reached 99.97% with 5 modes, confirming that this mode count adequately captures the vapor-liquid interface dynamics. Liquid fraction in the PCM region exhibited similar accuracy with 5 modes yielding 99.08% energy contribution. The POD-ROM demonstrated consistent accuracy across both Case A and Case B test scenarios, which explored different inlet conditions and time ranges. The relative mean error for temperature predictions remained below 0.1% in both cases, and melting time predictions showed errors within 4.7%. The consistency across test cases indicates good generalization capability of the POD basis.

 doi:10.20944/preprints202602.1504.v1

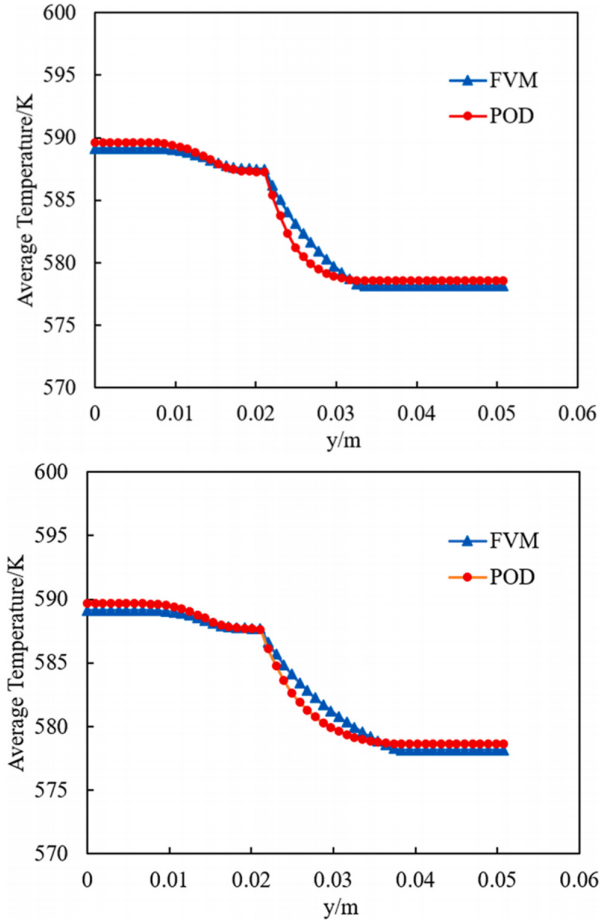

Figure 15. Finite volume model (FVM) and POD model comparison of the average temperature when $t = 0.5$ hours (left) and $t = 1$ hour (right) [8].

The intended application is fast simulation and control of thermal energy storage in DSG solar thermal power plants. In these systems, solar collectors generate steam that must be stored during periods of excess generation and retrieved during shortfalls. The POD-ROM enables rapid evaluation of storage performance under fluctuating solar input, supporting optimization of storage sizing, operating strategies, and dispatch scheduling. The computational efficiency is particularly valuable for model-based predictive control, where control decisions must be updated based on forecasted solar availability and electricity demand. The POD-ROM can be embedded in optimization algorithms that run in real-time or near-real-time, enabling closed-loop control that maximizes energy delivery or revenue while respecting system constraints.

The POD-ROM's primary limitation is its reliance on pre-computed snapshots covering the operating range of interest. Extrapolation beyond the parameter space sampled during training can produce inaccurate results, as the POD basis may not adequately represent physics outside the training domain. The model also inherits any inaccuracies in the underlying full-order model, including limitations of the Lee model and enthalpy-porosity approach. The interpolation-based approach for obtaining POD coefficients may introduce errors at intermediate operating conditions not well-represented in the snapshot database. More sophisticated interpolation methods or larger snapshot libraries could improve accuracy but at the cost of increased training effort. The model also provides only temperature, velocity, and phase fraction fields—derived quantities like local heat fluxes or stress distributions require post-processing. A practical limitation noted by the authors is the relatively small number of training samples (13 trajectories) used in this demonstration. While sufficient for the two-parameter space explored, more complex systems with additional degrees of freedom would require substantially more snapshots to adequately sample the solution manifold.

 doi:10.20944/preprints202602.1504.v1

The linear nature of POD may also limit accuracy for highly nonlinear phenomena like turbulent convection or complex phase change behavior.

5.4. Analytical 1D ROM for Metal-Polymer Composite Heat Exchangers

A ROM was proposed for a novel LHS system utilizing additively manufactured metal–polymer composite heat exchangers [2]. The physical configuration consists of metal fin-wires arranged in a tube-bank geometry, with the interstitial spaces filled by polymer encapsulating the PCM. This cross-media approach leverages additive manufacturing to create integrated structures where conductive metal fins enhance heat transfer while the polymer provides in-built macro-encapsulation for the PCM. The system geometry is reduced to a segment-level model comprising a single PCM-wire cylindrical domain based on the tube-bank arrangement. Each cylindrical domain represents the PCM wrapped around one metal wire, with the radius determined by the wire spacing (transverse pitch ST and longitudinal pitch SL). This geometric abstraction enables analysis of the fundamental heat transfer unit cell rather than the entire heat exchanger, dramatically reducing model complexity.

The ROM assumes one-dimensional radial conduction inside the PCM cylinders enveloping the metal wires, neglecting both axial conduction along the wire direction and convection in the liquid PCM. This simplification is justified for low Stefan number applications where conduction dominates and for geometries with high aspect ratios where radial resistance significantly exceeds axial resistance. The metal wire is treated as having infinite thermal conductivity in the axial direction but finite radial conductivity that couples to the PCM through the wire-PCM interface. Heat transfer from the heat transfer fluid to the PCM occurs through convective boundary conditions on the wire surface. The convective heat transfer coefficient is obtained from standard correlations for flow over heated cylinders in tube banks. The PCM phase change is modeled using thermal resistance and energy conservation principles, with latent energy analytically computed for the cylindrical domain and then time-integrated for the entire TES assembly. Notably, the model neglects sensible thermal capacity, making it applicable primarily for low Stefan number applications where latent heat dominates over sensible heat. The model also assumes negligible overlaps between adjacent PCM cylinders, though geometric studies were conducted to assess the impact of overlapping regions where this assumption breaks down.

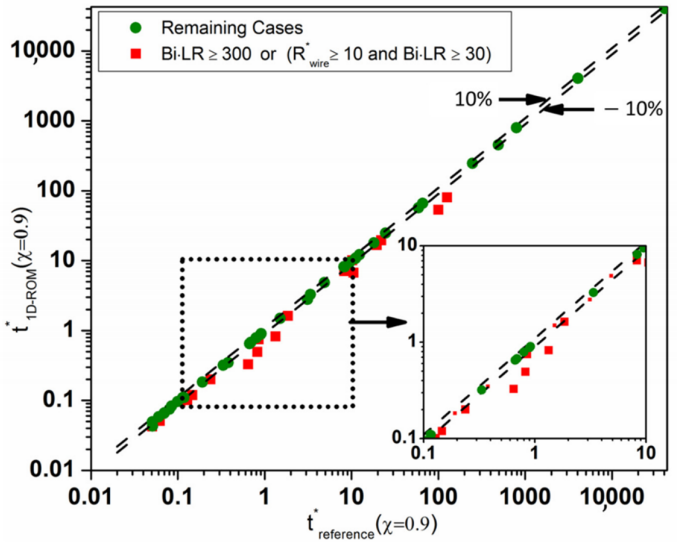

Figure 16. Correlation between 1D ROM and 2D CFD model [2].

 doi:10.20944/preprints202602.1504.v1

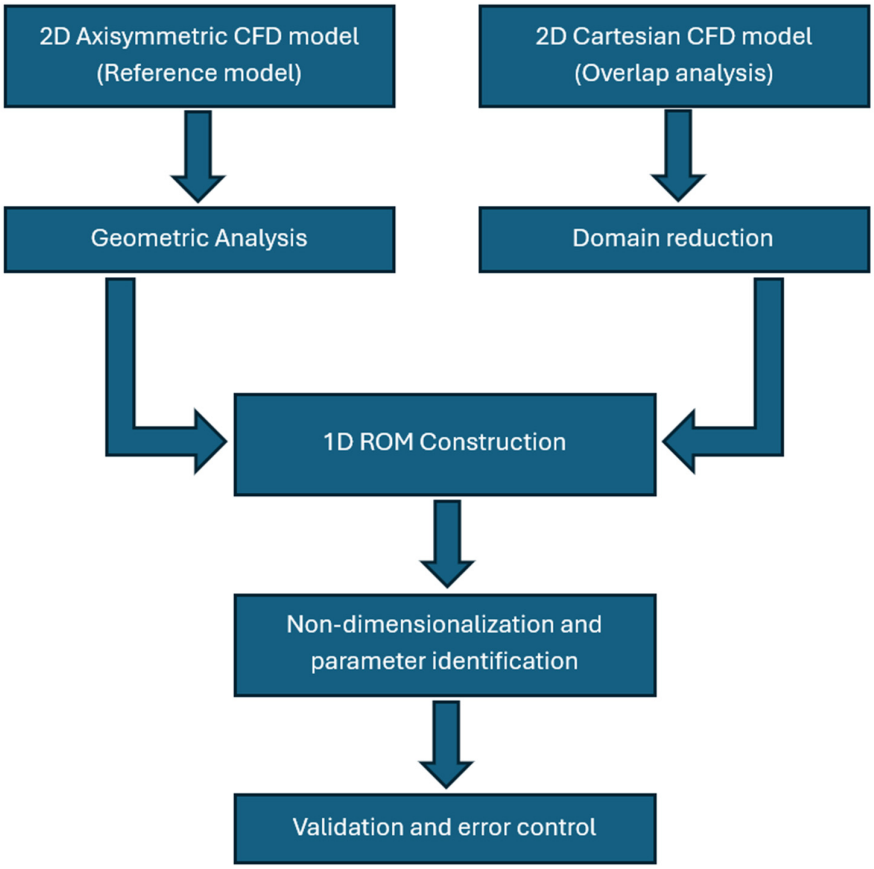

Figure 17. 1D ROM development flow for PCM-based TES [2].

The analytical ROM is constructed using thermal resistance and energy conservation principles rather than discretized differential equations. The heat flow from the HTF through the convective boundary layer, across the wire, and into the PCM is modeled as a series of thermal resistances. The melting process advances radially inward from the heated wire surface, with the position of the solid-liquid interface tracked as a function of time. Energy conservation applied to the moving phase boundary yields an ordinary differential equation for the interface position. This equation is solved analytically or semi-analytically, providing explicit expressions for the temperature distribution and interface location as functions of time. The total latent energy stored is obtained by integrating the energy released during solidification (or absorbed during melting) over the volume of PCM that has undergone phase change. The segment-level model is then extended to the entire TES by multiplying the energy stored in a single cylindrical domain by the total number of wire-PCM units. This scaling approach assumes all units behave identically, which is valid for uniform inlet conditions and negligible flow maldistribution. The computational cost is minimal since the ROM involves evaluating analytical or semi-analytical expressions rather than solving large systems of equations. The general workflow that transform the original multidimensional heat transfer problem into an efficient one-dimensional reduced-order formulation is presented in Figure 17.

Rather than training on high-fidelity simulation snapshots, the 1D ROM was validated against a 2D axisymmetric CFD model. The CFD model represents a single cylindrical PCM domain with radial and axial heat conduction, providing a reference solution against which the 1D assumption can be assessed. A 2D Cartesian CFD model was also developed to study the geometric behavior of overlaps between adjacent cylinders and their effect on model accuracy. The validation studies varied three non-dimensional parameters across wide ranges: (i) τ (dimensionless time, ranging from 0.03 to 300), (ii) BiLR (Biot number based on axial conductance, 0.03 to 300), and (iii) R_{wire} (resistance ratio, 0.01 to 100). These parameters characterize the relative importance of different heat transfer

 doi:10.20944/preprints202602.1504.v1

mechanisms and resistance components, allowing assessment of where the 1D approximation is valid. Optimum geometric ranges of wire spacings and sizes were identified through these parametric studies. Spacing ratios of ST/SL = 1.27 and 3.5 at higher r_{max} were found to yield accurate results. For most parameter combinations, the 1D ROM correlated well with the 2D axisymmetric reference model to within 10%, as shown in Figure 16, except at extreme ranges where BiLR ≥ 300 or $R_{wire} \geq 10$ led to significant axial conduction deviating from the 1D assumption.

The model order is characterized by a single spatial coordinate (radial position) with analytical or semi-analytical solutions obviating the need for discretization. The primary unknowns are the interface position as a function of time and the temperature distribution in the solid and liquid regions, which can be expressed in closed form or require solution of a single ordinary differential equation. Computational cost is not explicitly quantified in terms of speed-up factors or wall-clock times. However, the analytical nature of the model suggests near-instantaneous evaluation suitable for real-time applications or extensive design optimization studies. The model is particularly appropriate for design optimization problems where the ROM must be evaluated thousands or millions of times to identify optimal configurations.

The primary accuracy metric is the comparison of performance parameters (such as time to reach 90% melting) between the 1D ROM and the 2D CFD reference. For the ranges where the 1D assumption is valid, deviations remain within 10%. This accuracy is achieved without any tuning or calibration—the ROM is purely based on first principles with no adjustable parameters beyond standard material properties and heat transfer correlations. The geometric studies using 2D Cartesian CFD revealed that overlapped areas between adjacent cylindrical domains can introduce errors when their extent becomes significant. The model accuracy depends on selecting appropriate spacing ratios that minimize these overlaps while maintaining reasonable packing density. Optimal spacing ratios identified through these studies help guide practical system design. For extreme parameter combinations outside the validity range (BiLR ≥ 300, indicating dominant axial conduction in the wire), deviations can reach 86%. However, for typical applications with BiLR < 3 where fluid-side resistance dominates, the model unconditionally correlates well with 2D CFD regardless of Rwire value. This delineation of the validity domain helps users understand when the 1D ROM can be trusted.

The target application is peak-load shifting for building cooling through thermal energy storage. The lightweight, low-cost metal-polymer composite HX enables integration of latent heat storage in building HVAC systems, charging the PCM during off-peak hours when electricity is inexpensive and discharging during peak demand periods. The 1D ROM supports rapid design of these systems, determining optimal PCM selection, wire dimensions, and spacing. The model is also applicable to pulsed-power cooling applications where transient high heat loads must be managed. In such applications, the ROM enables assessment of how quickly the PCM can absorb heat pulses and how long before thermal management fails. The analytical nature makes the model suitable for parametric design studies exploring trade-offs between weight, volume, cost, and thermal performance.

The neglect of sensible thermal capacity limits applicability to low Stefan number situations where latent heat dominates. For PCMs with low latent heat or applications with large temperature excursions, the sensible heat contributions cannot be ignored. The assumption of 1D radial conduction breaks down when axial conduction becomes significant (large BiLR or R_{wire}), requiring users to verify they are operating within the valid parameter ranges. Natural convection in liquid PCM is neglected, which may underpredict heat transfer for materials with low viscosity and moderate to large wire diameters [6]. The model also assumes perfect thermal contact between the wire and PCM, whereas in reality interfacial thermal resistance may exist. Geometric overlaps between adjacent cylindrical domains are not rigorously accounted for, though their impact has been studied and optimal spacing ratios identified to minimize errors.

 doi:10.20944/preprints202602.1504.v1

5.5. CFD Results-Based Look-Up Table ROMs

A novel approach was introduced to generate reduced-order models for LHS systems with macro-encapsulated PCM, utilizing CFD simulation results as the basis [9]. The physical system consists of spherical capsules filled with PCM arranged in layers within a storage tank. Hot HTF flows upward through the tank, charging the PCM by melting it through convective heat transfer at the capsule surfaces and conductive/convective heat transfer within each capsule. The ROM approach focuses on a single capsule as the fundamental modeling unit, recognizing that system behavior emerges from the collective response of many such capsules. This segment-level reduction is analogous to the approach taken by Kailkhura et al. [2], but here the detailed capsule dynamics are captured through comprehensive CFD simulations rather than analytical approximations. Three levels of modeling fidelity were explored: (1) PCM only (CFD-PCM), (2) PCM with air gap and capsule wall (CFD-PCM-air-wall), and (3) full system including surrounding HTF (CFD-PCM-air-wall-HTF).

The CFD models capture detailed heat transfer physics within and around individual PCM capsules. The PCM phase change is modeled using the enthalpy-porosity method, which naturally handles the moving solid-liquid interface and allows for mushy zone formation. Close-contact melting (CCM) at the bottom of the capsule—where the liquid PCM layer becomes very thin as solid PCM sinks due to gravity—is resolved by the CFD mesh. Natural convection within liquid PCM is fully captured through solution of the Navier-Stokes equations coupled with energy conservation. The Boussinesq approximation relates density variations to temperature differences, driving buoyancy-induced flow. This convection significantly affects melting rates, particularly in the later stages of charging when large liquid regions have formed. For the models including the capsule wall, conjugate heat transfer across the shell is resolved, accounting for thermal resistance and capacitance of the wall material. The CFD-PCM-air-wall-HTF variant further includes the HTF flow field around the capsule, capturing the development of thermal boundary layers and wake effects that influence heat transfer coefficients. Each level of fidelity adds computational cost but potentially improves prediction accuracy.

The ROM methodology consists of two stages: (1) offline CFD simulation campaign to populate look-up tables, and (2) online rapid evaluation using the tables within a system simulation model. In the offline stage, detailed CFD simulations of a single capsule are performed for systematically varied boundary conditions. The results are written into look-up tables that contain the charging power of one capsule as a function of the enthalpy stored and the boundary conditions (HTF temperature, heat transfer coefficient or mass flow rate). The look-up tables effectively compress the CFD results into a functional relationship $Q = f(H, T_{HTF}, k \text{ or } \dot{m})$, where Q is the instantaneous heat transfer rate, H is the total enthalpy stored in the capsule, and the remaining arguments characterize the thermal driving force and convection strength. This representation captures the essential nonlinear relationship between driving conditions and heat transfer without requiring solution to the full CFD problem. In the online stage, the system simulation model discretizes the storage tank into layers, with each layer containing multiple capsules. At each time step, the enthalpy of capsules in each layer is known, allowing the look-up table to be queried to determine the heat transfer rate. This rate is used to update the enthalpy and HTF temperature, marching forward in time. The approach assumes capsules within a layer behave identically and neglects inter-layer heat transfer, which are reasonable approximations for most storage configurations.

 doi:10.20944/preprints202602.1504.v1

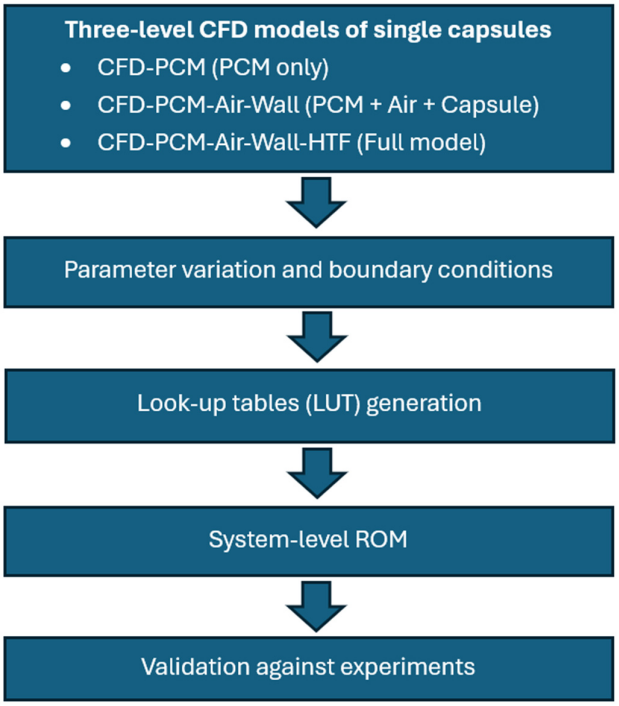

Figure 18. LUT ROM development for LHS system with macro-encapsulated PCM [9].

The offline CFD simulations were performed for 6-18 different combinations of boundary conditions depending on the model variant. The parameters varied included HTF temperature (22.5-35°C), heat transfer coefficient (114-285 W/m²K for fixed coefficient models), and mass flow rate (5.893-7.237 kg/min for the HTF-included model). Each CFD simulation tracked one capsule from the fully solid state through complete melting, providing time series of heat transfer rate and stored enthalpy. Each individual CFD simulation lasted up to more than two weeks on one CPU core of a workstation. This substantial computational investment is incurred once during the offline training phase, but the resulting look-up tables enable thousands of rapid online evaluations. The approach is viable when access to computing clusters allows many simulations to run in parallel, amortizing the wall-clock time for training data generation. The CFD mesh for the PCM domain contained 60,000 cells with strong refinement near the bottom boundary to resolve close-contact melting. Mesh independence studies confirmed this resolution adequately captures the essential physics without excessive computational cost. The CFD models were implemented in OpenFOAM and validated against experimental measurements before use in training data generation. The transformation of extensive CFD training simulations into an ultra-fast look-up table reduced-order model is summarized in Figure 18.

The look-up table (LUT) ROM has no explicit state variables in the traditional sense—it operates by table interpolation rather than solving differential equations. The effective model complexity is determined by the resolution of the look-up table grid, which spans 2-3 dimensions depending on whether a constant heat transfer coefficient or varying mass flow rate is considered. The tables are queried using efficient interpolation functions, with computational cost dominated by table read operations. The computational speed-up achieved is extraordinary. The fastest ROM variant completed system simulations in approximately 5 seconds, while the reference CFD simulation of the full storage would take up to two weeks. This represents a speed-up factor of approximately 80,000×, among the highest reported for any LHS ROM. Even accounting for time spent reading from look-up tables—which can be further optimized by compiling to C code—the speed-up factor remained above 50,000×.

 doi:10.20944/preprints202602.1504.v1

The ROM was validated against experimental measurements from a two-layer storage system. The temporal mean deviation of energy content between experiments and the ROM was only 5%, demonstrating excellent agreement despite the multiple simplifications inherent in the segment-level approach. This validation included realistic effects like heat losses and non-uniform HTF distribution that are challenging to capture in simplified models. Comparisons between the three model variants revealed that including the capsule wall is essential for accurate predictions, especially when wall thermal conductivity is significantly higher than PCM conductivity. The HTF flow field, however, can be replaced by a properly defined convective boundary condition without substantial loss of accuracy, simplifying the CFD training simulations. These findings provide guidance on the minimum level of physics fidelity required.

The intended application is rapid design and optimization of large-scale LHS systems with macro-encapsulated PCM. The ROM enables evaluation of different capsule sizes, materials, and tank geometries across varying operating conditions. The speed-up makes it feasible to simulate full charge-discharge cycles over days or weeks, supporting techno-economic analysis and control strategy development.

The primary limitation is the substantial upfront computational cost for CFD training data generation, requiring access to computing clusters for parallel execution. The approach is most valuable when many design iterations or long-duration simulations justify this investment. The look-up tables are specific to the capsule geometry and materials studied—new configurations require new CFD campaigns. Additionally, the model assumes uniform behavior within each tank layer and neglects potential flow maldistribution or hot spots that could occur in large storage systems.

5.6. Machine Learning-Based Reduction: Artificial Neural Networks for Finned Enclosures

Just recently, the PCM melting dynamics in a rectangular enclosure with dimensions of 50 × 50 mm was predicted using artificial neural networks (ANN) [126]. The configuration includes a 5 mm thick aluminum heater plate maintained at constant temperature (70°C) on the left side. Inside the enclosure are two fins with varying lengths of 12.5 mm, 25 mm, and 37.5 mm, allowing investigation of fin geometry effects on melting behavior. The physical scope encompasses the solid-liquid phase change process and the evolution of the melting front over time. The numerical model accounts for the phase change process of PCM through energy conservation and momentum equations. The enthalpy-porosity method is employed to treat the mushy zone as a porous medium during melting, equating the liquid phase volume fraction to the porosity. The model captures heat conduction in both solid and liquid phases, natural convection effects during melting, and the temporal evolution of the solid-liquid interface. These governing equations provide the basis for generating training data through numerical simulation. The data-driven workflow that converts numerical simulation outputs into machine learning-informed ROM is outlined in Figure 19.

 doi:10.20944/preprints202602.1504.v1

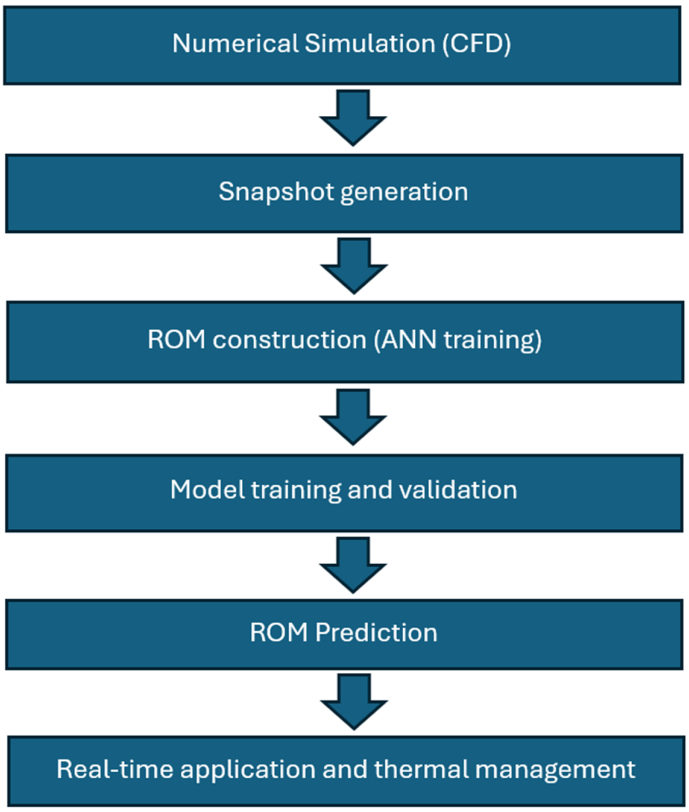

Figure 19. ML-informed ROM development workflow for predicting the melting time of PCM-based LHS system [126].

The ROM methodology employs ANNs trained on numerical simulation data. Spatial coordinate data of the solid-liquid interface at various time steps extracted from numerical contours are used to train the ANN model. The ANN learns the dynamic melting behaviors of PCM under varying conditions, subsequently enabling prediction of melting front evolution and temperature distribution. This represents a data-driven surrogate modeling approach that replaces expensive numerical simulations. The training approach uses coordinate data extracted from numerical simulation results at three different fin lengths (12.5 mm, 25 mm, and 37.5 mm). After training on these three geometries, the ANN model is employed to predict melting behavior at intermediate fin lengths of 20 mm and 30 mm, which were not included in the training dataset. This strategy tests the ANN's ability to interpolate across the geometric parameter space and predict results for conditions not explicitly simulated during training. The computational speedup achieved by the ANN approach is dramatic. Simulating PCM melting for two intermediate fin length cases (20 mm and 30 mm) via traditional numerical methods requires approximately 6 days of computational time. In contrast, the trained ANN model completes predictions in just a few minutes, representing a computational acceleration of roughly 1,440× while maintaining high accuracy. This substantial reduction enables rapid thermal system design exploration and optimization. The ANN model demonstrates exceptional accuracy with low error metrics. For PCM melting front training, mean absolute error (MAE), mean squared error (MSE), and Pearson's correlation coefficient (R) values are approximately 0.014, 0.03, and 0.99, respectively. For temperature distribution, corresponding metrics are around 0.016, 0.03, and 0.99. Validation on unseen fin lengths (20 mm and 30 mm) yields MAE, MSE, and R values of approximately 0.02, 0.03, and 0.98, demonstrating robust generalization. Graphical comparisons show predicted melting fronts and temperature distributions closely aligned with numerical simulation results across all time intervals. The ANN approach is intended to advance thermal management system designs through efficient prediction of PCM melting behavior. By reducing simulation time from approximately 6 days to a few minutes with high accuracy, the

 doi:10.20944/preprints202602.1504.v1

methodology enables practical design optimization of finned PCM enclosures. The approach is adaptable to various thermal management applications where rapid performance assessment is required during iterative design processes. While the ANN model shows high accuracy for interpolation within the training parameter range, the study does not extensively explore extrapolation beyond the geometric range covered by the three training cases. The reliance on numerical simulation data for training introduces the same physical assumptions inherent in the CFD approach. Additionally, the transferability of the trained model to different enclosure sizes, fin materials, or PCM types requires validation and potentially retraining.

5.7. Machine Learning-Based Reduction: XGBoost for Triplex-Tube Systems

Another study developed a machine learning prediction method for a triplex-tube thermal energy storage system incorporating PCM with Y-shaped fins to enhance heat transfer [127]. The configuration includes design variables encompassing fin angle (10-20°), fin width (5-15 mm), fin design characteristics, and operational conditions including heat transfer fluid temperature (60°C). The physical scope encompasses the melting response time of PCM, representing the duration required for complete or substantial phase transition under specified thermal conditions. The numerical model is based on the enthalpy-porosity method for simulating the melting process. The governing equations include the continuity equation, momentum equations with Boussinesq approximation for natural convection, and energy conservation accounting for phase change latent heat. The liquid fraction of PCM is calculated as a function of temperature relative to phase change limits, and the mushy zone constant is a key element controlling the transition. The model also accounts for boundary conditions where no-slip conditions are applied at solid surfaces. Four machine learning algorithms were employed to predict melting response time: polynomial regression, support vector regression (SVR), random forest (RF) regression, and extreme gradient boosting (XGBoost). Hyper-parameter optimization was performed using a Bayesian approach to refine each model's performance. The XGBoost model demonstrated superior predictive capability compared to alternative approaches, emerging as the optimal model class for this prediction task. The training dataset comprises 60 numerical simulation cases with melting response times ranging from 15 to 45 minutes under varying design and operational conditions. Prior to model development, variable independence was validated to ensure robust predictions. The dataset encompasses variations in fin angle, fin width, and heat transfer fluid temperature, capturing the interaction effects between these design parameters on system response time. The trained XGBoost model achieves 92% accuracy in predicting melting response time. The general workflow for developing the ML-informed ROM model is presented in Figure 20.

 doi:10.20944/preprints202602.1504.v1

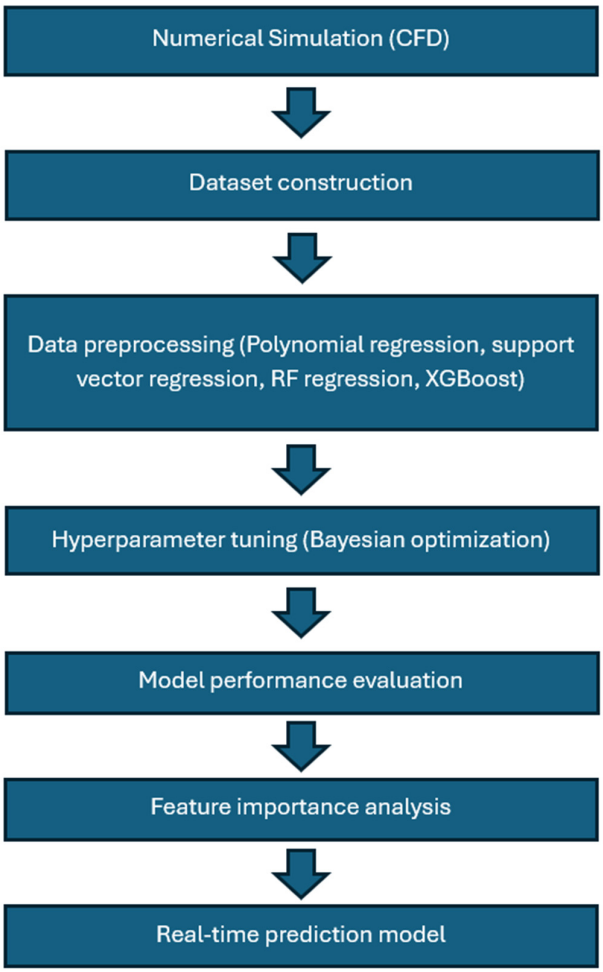

Figure 20. XGBoost model (ML-informed ROM) development for triplex-tube TES [127].

By replacing expensive numerical simulations with rapid ML predictions, the approach enables efficient design space exploration. Once trained, the model can evaluate numerous design candidates in minimal computational time compared to full numerical simulations, substantially accelerating the design optimization process for triplex-tube thermal storage systems. Performance evaluation employed mean squared error and coefficient of determination (R^2) as primary metrics. The XGBoost model outperforms alternative algorithms, achieving the highest accuracy and lowest prediction error. In contrast, support vector regression exhibits significant overfitting in the testing set, highlighting the importance of appropriate model selection. The study demonstrates that XGBoost provides reliable predictions for melting response time across the tested parameter space. The methodology enables quantitative prediction of melting response time for novel triplex-tube thermal energy storage systems. Accurate prediction of melting response time is vital for optimizing thermal energy storage systems, which play key roles in addressing temporal mismatch between thermal energy demand and supply in built environments. The identified relationships between design parameters and response time can guide fin geometry optimization for enhanced thermal performance. Feature importance analysis revealed that fin width and heat transfer fluid temperature are dominant factors, contributing 51% and 47% to prediction variance, respectively, while fin angle has marginal influence at 2%. The study does not extensively explore extrapolation beyond the 15-45 minute melting response time range or variations in PCM properties substantially different from those used in training. Additionally, the transferability of the trained model to different triplex-tube configurations or alternative PCM materials requires validation through additional simulations.

 doi:10.20944/preprints202602.1504.v1

5.8. Summary and Comparative Analysis of ROMs for PCM-Based LHS Systems

The reviewed ROMs for PCM-based latent heat storage systems span five major reduction philosophies: physics-reduced analytical models, grey-/black-box metamodels, projection-based POD models, CFD-results–based look-up tables, and purely data-driven machine learning surrogates, each reducing computational cost in fundamentally different ways while retaining varying levels of physical fidelity. Analytical and two-temperature porous-medium ROMs simplify governing equations through dimensional reduction and thermal resistance analogies, yielding very low model order and high interpretability but limited geometric flexibility and validity ranges. Grey-box ε-NTU and black-box Kriging metamodels remove spatial resolution entirely and rely on training from finite-volume data to predict global performance metrics, achieving 18×–220× speed-ups with sub-Kelvin errors and strong suitability for system-level simulations. POD-based ROMs compress full CFD spatial fields into a few dominant modes, preserving temperature and phase distributions with over 300× acceleration and <0.1% error, making them ideal for control and digital twin applications but dependent on representative snapshot databases. CFD look-up table ROMs precompute detailed capsule physics offline and replace online PDE solving with table interpolation, producing extreme speed-ups (~80,000×) at the expense of large upfront CFD cost and geometry specificity. In contrast, ANN and XGBoost surrogates learn melting dynamics and response times directly from CFD data, enabling ~1,440× acceleration and high statistical accuracy for complex finned and triplex-tube geometries, though with limited extrapolation capability and reduced interpretability. Collectively, these approaches demonstrate a trade-off between interpretability, transferability, data dependence, and computational speed, indicating that ROM selection must be aligned with the intended application, whether for design optimization, system simulation, control, or geometric exploration.

Table 1 provides a comparative overview of representative ROMs developed for LHS systems, highlighting the diversity of modeling philosophies, physical fidelity, and computational performance. The reported ROMs span a wide range of configurations, from packed-bed spherical capsule systems modeled using two-temperature non-equilibrium formulations [82] to PCM-embedded heat exchangers represented by both data-driven kriging metamodels and ε-NTU–based semi-analytical approaches [1], as well as fully ML-based reduction models [126,127]. While physics-based ROMs, such as the two-temperature enthalpy model and 1D thermal resistance networks, preserve explicit representations of conduction and latent heat effects, their computational speed-up is either limited or not explicitly quantified, and their accuracy may degrade to around 10% in composite heat exchanger applications [2]. In contrast, surrogate and interpolation-based ROMs, including kriging, POD interpolation, and CFD-derived look-up tables, demonstrate significantly higher computational acceleration, with reported speed-ups ranging from 18× up to 80,000×, while maintaining acceptable thermal prediction accuracy [1,8,9,126,127]. Notably, POD-based interpolation applied to shell-and-tube direct steam generation (DSG) systems achieves sub-percent relative mean error with over 300× speed-up [8], while surrogate-assisted optimization of PCM-based plate heat exchangers attains more than 90% computational savings in identifying Pareto-optimal designs across large geometric design spaces illustrating the potential of projection-based ROMs for large-scale solar thermal applications. Overall, the results summarized in Table 2 indicate a fundamental trade-off between physical interpretability and computational efficiency: physics-based ROMs offer transparency and robustness, whereas data-driven and hybrid ROMs deliver the extreme speed-ups required for large-scale design optimization, digital twins, and real-time control of PCM-based LHS systems.

 doi:10.20944/preprints202602.1504.v1

Table 2. Summary of ROMs for LHS systems for the past five years

ROM Method	LHS Configuration	Physics	Error/ Accuracy	Speed-up	Application
Two-temperature non-equilibrium [82]	Packed bed spherical capsules	Conduction + enthalpy method	2.5 K (max)	Not reported	Solar thermal storage
Kriging metamodel (Black-box) [1]	PCM-embedded HX	Heat transfer (metamodel)	0.05 K (MAE)	220×	TES device design
ε-NTU method (Grey-box) [1]	PCM-embedded HX	Heat transfer (ε-NTU)	0.10 K (MAE)	18×	TES device design
POD interpolation [8]	Shell-tube DSG-STP	Conduction + convection + Lee model	<0.1% (RME)	314×	DSG solar thermal power
1D analytical thermal resistance [2]	Metal-polymer composite HX	1D radial conduction	10% (validation)	Not reported	Peak-load shifting
CFD look-up table [9]	Macro-encapsulated spherical	Conduction + CCM + convection	5% (energy)	80,000×	LHS design
Artificial Neural Network [126]	PCM Rectangular Enclosure	Enthalpy-porosity method	MAE: 0.02, R^2: 0.98	~2,000×	Finned PCM thermal storage
XGBoost [127]	Triplex-tube TES	Enthalpy-porosity method	92% accuracy	Not reported	TES device melting prediction

Figure 21 illustrates the wide range of reported computational speed-ups achieved by different reduced-order modeling strategies applied to LHS systems, highlighting the strong dependence of performance on the underlying ROM paradigm. Surrogate-based and database-driven approaches exhibit the most dramatic acceleration, as demonstrated by the CFD look-up table model [9], which reduces a two-week transient simulation to approximately 5 seconds, corresponding to an extraordinary speed-up of nearly 80,000×. Projection-based ROMs provide a more moderate but still substantial improvement: the POD-interpolation model [8] accelerates a high-fidelity shell-and-tube DSG simulation from 4 hours to 46 seconds, achieving a speed-up of 314× while maintaining sub-percent error levels. In contrast, semi-empirical and meta-modeling approaches such as the kriging-based PCM heat exchanger model [1] deliver more limited acceleration (approximately 18×), reflecting the additional overhead associated with regression and response surface evaluation. Collectively, Figure X reveals a clear hierarchy in computational efficiency, with data-driven surrogates and precomputed databases enabling near real-time evaluation of PCM-based LHS systems, whereas projection-based ROMs offer a balanced trade-off between accuracy and computational tractability for dynamic simulation and control-oriented applications.

 doi:10.20944/preprints202602.1504.v1

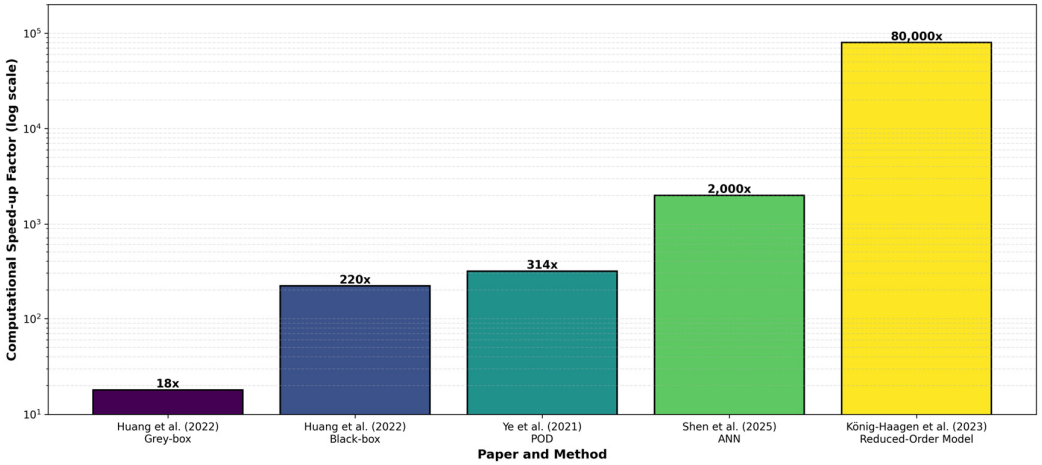

Figure 21. Computational speed-up across ROMs for LHS systems with reported speed-up factors.

A clear pattern emerges from comparing these approaches:

- Physics-based ROMs [2,82] reduce dimensionality of the governing equations and offer transparency and robustness but limited geometric flexibility.
- Metamodel and grey/black-box ROMs [1] eliminate spatial resolution and are ideal for system coupling and optimization.
- Projection-based ROMs [8] retain spatial fidelity with significant compression, making them attractive for control and digital twins.
- CFD look-up ROMs [9] trade enormous offline cost for extreme runtime speed.
- Machine learning ROMs [126,127] bypass physics reduction entirely and learn behavior directly from data, enabling rapid prediction for complex geometries.

These methods also reveal a trade-off between interpretability, transferability, and computational speed. Analytical and physics-based models are transferable but slower than ML and look-up approaches. ML and look-up ROMs are extremely fast but geometry-specific and dependent on training data. POD offers a balance by preserving fields with moderate data needs but suffers from extrapolation limits. Figure 22 visualizes the trade-off between interpretability and computational speed across ROM categories. Physics-based ROMs offer high interpretability but modest speed-up; data-driven surrogates achieve extreme acceleration at the cost of interpretability and transferability; projection-based methods occupy a middle ground, preserving spatial fields with moderate speed-up.

 doi:10.20944/preprints202602.1504.v1

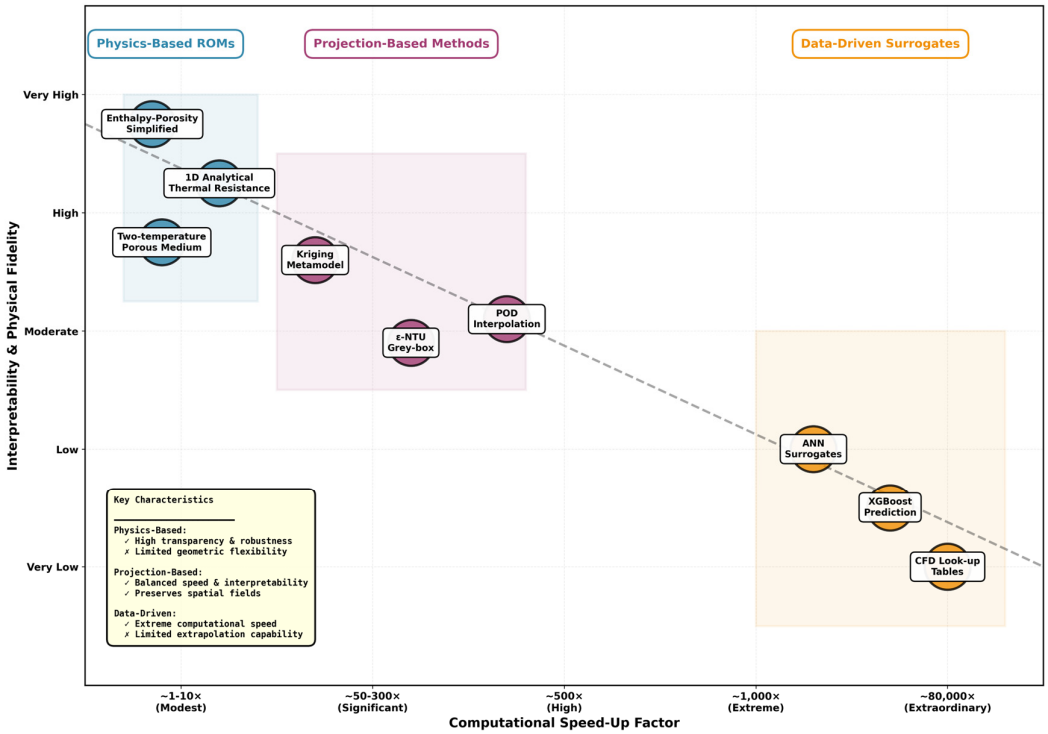

Figure 22. Trade-off between interpretability and computational speed across ROM categories

From an application standpoint, different ROM philosophies naturally align with specific PCM-based latent heat storage configurations. In solar thermal packed-bed systems, the two-temperature porous medium ROM is particularly suitable because it captures the non-equilibrium heat exchange between the heat transfer fluid and encapsulated PCM while maintaining low computational cost [82]. For HVAC-integrated PCM heat exchangers, Kriging metamodels and ε-NTU–based grey-box ROMs are effective due to their ability to predict global heat exchanger performance metrics without resolving spatial fields, making them ideal for system-level building simulations [1]. In solar direct steam generation (DSG) systems, especially for control and transient response analysis, POD-based ROMs are preferred because they retain spatial temperature and phase information while achieving significant model compression and real-time capability [8]. For large macro-encapsulated PCM storage tanks, CFD-results–based look-up table ROMs provide an efficient solution by replacing online PDE solving with interpolation of precomputed high-fidelity capsule data [9]. In geometrically complex configurations such as finned enclosures and triplex-tube heat exchangers, ANN and XGBoost surrogates perform well because they learn highly nonlinear melting dynamics directly from CFD datasets across varied geometric parameters [126,127]. Meanwhile, for additively manufactured composite heat exchangers, simplified analytical one-dimensional ROMs based on thermal resistance networks remain attractive due to their transparency, low order, and ease of integration into design workflows [2].

Overall, the comparative analysis shows that there is no single best ROM for PCM-based LHS. The optimal choice depends on whether the goal is design optimization, system simulation, control, or geometric exploration. The field is progressively moving toward hybrid approaches where physics-based structure is combined with machine learning flexibility, indicating a future direction where ROMs retain physical consistency while achieving the extreme computational efficiency required for real-time applications.

Although the studies surveyed above demonstrate promising strategies for reducing computational expense in PCM-based LHS systems, they also reveal persistent challenges that motivate the future research directions, which are outlined in Section 6.

 doi:10.20944/preprints202602.1504.v1

6. Challenges and Future Directions

Despite the advancements in ROMs for LHS systems, several critical challenges remain, highlighting the need for future research on their development and integration. These challenges span computational accuracy, model generalization, experimental validation, system integration, and the incorporation of emerging technologies.

6.1. Model Fidelity, Accuracy, and Efficiency Trade-Offs

A fundamental challenge in ROM development is balancing computational speed with simulation accuracy [1]. While ROMs achieve significant speed-ups, maintaining acceptable accuracy across operating conditions remains problematic. The trade-off becomes particularly acute for nonlinear time-dependent dynamics, where conventional techniques like the Reduced Basis method lack efficiency despite rigorous construction [128]. Scalability adds another dimension: large-scale LHS systems integrating hundreds of PCM modules require ROMs that remain tractable while accounting for geometric complexities such as finned tubes, wavy channels, and conical structures [129–133]. Selecting the appropriate reduction strategy—POD, deep autoencoders, or hybrid approaches—depends on problem-specific characteristics and is not straightforward. The optimal balance between compression and preservation of essential dynamics, particularly for systems with complex spatial and temporal variations, remains an open research question [128].

6.2. Data Requirements, Quality, and Generalization

Machine learning-based ROMs require large, comprehensive training datasets, which are often unavailable for thermal applications [134]. Generating optimal full-order snapshots is computationally intensive, with some CFD simulations lasting weeks [9]. This offline burden creates a barrier to robust ROM development, as generating sufficient data for varied operating conditions and geometric configurations becomes prohibitively expensive. Furthermore, the interpretability of ML-based ROMs remains a concern, particularly in safety-critical applications [134]. Black-box models make it difficult to understand underlying physics and build confidence in predictions. Generalization beyond training domains poses significant challenges; models trained on specific parameter ranges may not perform reliably when extrapolated to new conditions [134]. Ensuring that ROMs trained on limited data accurately predict behavior across the full range of real-world scenarios requires careful design space selection and sampling techniques [1].

6.3. Physics Integration and Multi-Physics Phenomena

Developing ROMs that accurately capture complex multi-physics phenomena—phase change, natural convection, conjugate heat transfer—remains challenging [135]. The modeling community is actively addressing complexities associated with multi-phase interactions, aiming to enhance simulation accuracy. Boundary condition treatment requires significant attention: most numerical models of macro-encapsulated PCM do not include the heat transfer fluid or capsule wall and rarely pay special attention to boundary conditions [9]. Determining whether the capsule wall and HTF must be included in CFD models for ROM development remains an open question. Few publications explicitly indicate the impact of reduced-order PCM heat exchanger modeling on system-level accuracy, highlighting the need for more comprehensive studies evaluating ROM performance within complete thermal energy storage systems [1].

6.4. Validation, Standardization, and Real-World Deployment

A significant gap exists between numerical ROM development and experimental validation. Latent heat TES experiments are difficult, and numerical simulation alone cannot meet engineering application needs [8]. More pilot plants for testing PCM integrated with solar-powered thermal industrial processes should be performed, as operating conditions fluctuate in time, requiring specific studies for charging and discharging cycles [136]. The high costs associated with high-temperature

 doi:10.20944/preprints202602.1504.v1

PCM experimentation, both at laboratory and pilot scales, and the difficulty in ensuring identical initial conditions across thermal cycles compound this challenge [137].

Integration with real-time control systems represents a significant future direction. LHS systems coupled with intermittent renewable sources require precise control of charging and discharging cycles for optimal performance and grid stability [138–140]. Developing ROMs suitable for model predictive control (MPC), where rapid solution of parameterized optimal control problems is essential, remains computationally demanding. Ensuring ROM robustness under varying operating conditions—fluctuating HTF temperatures and flow rates, material property variations, degradation over time—remains a challenge [141].

Material characterization over extended operational periods is fundamental. Stability and corrosion problems become more serious for inorganic salts and metals at storage temperatures above 100°C [142]. Performance degradation due to microstructural or chemical changes after multiple cycles affects ROM reliability. Long-term cycling stability tests under different operational conditions are needed to understand how material property changes affect ROM predictions [137].

Finally, the lack of standardized methodologies for ROM development, testing, and comparison hinders progress [134]. The absence of international standard methods for PCM testing creates inconsistencies in reported thermophysical and economic characteristics, making reliable ROM development difficult [143]. Establishing unified frameworks for ROM validation—including standardized test cases and performance metrics—would enable meaningful comparisons between different modeling approaches and accelerate best practice development. This standardization should extend to reporting requirements, ensuring future publications explicitly document computational costs, accuracy metrics, and validation ranges.

7. Conclusions

This review has comprehensively examined the landscape of reduced-order modeling (ROM) for phase change material (PCM)-based latent heat thermal energy storage (LHS) systems. The compelling need for ROMs is rooted in the fundamental computational bottleneck posed by high-fidelity simulations of nonlinear phase change phenomena, a critical barrier to the design, optimization, and real-time management of these technologies. We have detailed a wide array of ROM methodologies, from classical physics-intrusive techniques—linear projection-based methods (POD, RB) and nonlinear hyper-reduction strategies (DEIM, GNAT)—to contemporary non-intrusive, data-driven paradigms (DMD, Neural Networks, Autoencoders, GPs).

The critical synthesis of this review, particularly through the comparative analysis in Section 5.2, reveals a core trade-off matrix that must guide a researcher's choice of ROM. Interpretability and physical consistency are the strengths of physics-based ROMs (Sections 3.1 & 3.2), making them indispensable for applications demanding trust and insight, such as controller design and digital twins. Conversely, computational speed and geometric flexibility are the hallmarks of data-driven surrogates (Section 3.3), offering unparalleled efficiency for large-scale design optimization and system-level simulation. This matrix is further defined by the axis of data dependency and generalizability: while machine learning ROMs can achieve astonishing speed-ups (e.g., 80,000×), they require extensive, costly training data and often fail to extrapolate, whereas analytical or physics-reduced models offer broader robustness within their validity ranges with minimal training.

The case studies across diverse configurations—packed beds, shell-and-tube, and plate heat exchangers—confirm that no single ROM is universally optimal. Instead, the method must be matched to the application objective. For rapid parametric exploration of a fixed geometry, a black-box Kriging model may be ideal. For tracking spatial temperature fields in a controlled storage unit, a POD-based ROM is more suitable. For optimizing complex finned geometries, an ANN surrogate trained on CFD data provides the necessary speed.

Despite significant advances, critical challenges persist. The inherent nonlinearity of phase change, the dynamics of moving boundaries, and multi-timescale behavior continue to strain traditional ROM frameworks. The field grapples with the "curse of dimensionality" in training data

 doi:10.20944/preprints202602.1504.v1

acquisition, the limited interpretability of many ML-based ROMs, and a pressing need for rigorous experimental validation, especially for high-temperature applications.

Therefore, the most promising future of ROMs for LHS lies not in the exclusive advancement of one paradigm, but in the development of intelligent hybrid approaches. These hybrids seek to marry the physical consistency and generalizability of first-principles models with the adaptive efficiency and flexibility of machine learning. Examples include physics-informed neural networks (PINNs), ML-augmented closure models for POD-Galerkin systems, and symbolic regression to discover simplified governing equations from data. Progress also hinges on establishing standardized benchmarking protocols, creating robust strategies for uncertainty quantification, and fostering closer collaboration between computational modelers and experimentalists to generate the high-quality validation data essential for the next generation of ROMs.

By navigating the revealed trade-offs and pursuing these integrated research directions, ROMs will solidify their role as an indispensable enabling technology. They are key to accelerating the development, optimization, and deployment of efficient, cost-effective latent heat storage solutions, ultimately supporting the integration of renewable energy and the transition to a sustainable energy future.

Abbreviations

The following abbreviations are used in this manuscript:

ANN – Artificial Neural Network
BiLR – Biot number based on axial conductance ratio
CFD – Computational Fluid Dynamics
CFD-PCM – CFD model including PCM domain only
CFD-PCM-air-wall – CFD model including PCM, air gap, and capsule wall
CFD-PCM-air-wall-HTF – CFD model including PCM, air gap, capsule wall, and HTF flow
DEIM – Discrete Empirical Interpolation Method
DSG – Direct Steam Generation
DSG-STP – Direct Steam Generation Solar Thermal Power
FOM – Full-Order Model
FVM – Finite Volume Method
GNAT – Gauss–Newton with Approximated Tensors
GP – Gaussian Process
HTF – Heat Transfer Fluid
HVAC – Heating, Ventilation, and Air Conditioning
HX – Heat Exchanger
LHS – Latent Heat Storage
MAE – Mean Absolute Error
MAPE – Mean Absolute Percentage Error
ML – Machine Learning
MSE – Mean Squared Error
NTU – Number of Transfer Units
PCA – Principal Component Analysis
PCM – Phase Change Material
PINN – Physics-Informed Neural Network
POD – Proper Orthogonal Decomposition
RME – Relative Mean Error
RF – Random Forest
ROM – Reduced-Order Model
SVD – Singular Value Decomposition
SVR – Support Vector Regression

 doi:10.20944/preprints202602.1504.v1

TES – Thermal Energy Storage
ε-NTU – Effectiveness–Number of Transfer Units method
XGBoost – Extreme Gradient Boosting

References

1. Huang, R.; Mahvi, A.; Odukomaiya, W.; Goyal, A.; Woods, J. Reduced-Order Modeling Method for Phase-Change Thermal Energy Storage Heat Exchangers. *Energy Convers. Manag.* **2022**, *263*, 115692, doi:10.1016/j.enconman.2022.115692.
2. Kailkhura, G.; Mandel, R.; Shooshtari, A.; Ohadi, M. A 1D Reduced-Order Model (ROM) for a Novel Latent Thermal Energy Storage System. *Energies (Basel).* **2022**, *15*, 5124, doi:10.3390/en15145124.
3. Hai, T.; Omar, I.; Alizadeh, A.; Varshney, N.; Dixit, S.; Sultan, A.J.; Anqi, A.E.; Bhatnagar, S.; Rajab, H.; Singh Sawaran Singh, N. Optimization of Nano-Finned Enclosure-Shaped Latent Heat Thermal Energy Storage Units Using CFD, RSM, and Enhanced Hill Climbing Algorithm. *Sci. Rep.* **2025**, *15*, 12486, doi:10.1038/s41598-025-96599-y.
4. Nikolaev, P.; Jivkov, A.P.; Fifre, M.; Sedighi, M. Peridynamic Analysis of Thermal Behaviour of PCM Composites for Heat Storage. *Comput. Methods Appl. Mech. Eng.* **2024**, *424*, 116905, doi:10.1016/j.cma.2024.116905.
5. Lu, B.; Zhang, Y.; Sun, D.; Wang, C.; Wang, Z.; Luo, M. Improving the Melting Performance of Phase Change Material (PCM) in a Latent Heat Thermal Energy Storage Unit via a Non-Uniform Arrangement of Longitudinal Fin. *Proceedings of the Institution of Mechanical Engineers, Part A: Journal of Power and Energy* **2023**, *237*, 1100–1112, doi:10.1177/09576509231156236.
6. Sharif, S.; Walvekar, R.; Khalid, M.; Vaka, M.; Mubarak, N.M. Analysis of Melting Dynamics and Parametric Optimization in Encapsulated Phase Change Materials for Thermal Energy Storage. *ECS Journal of Solid State Science and Technology* **2024**, *13*, 013007, doi:10.1149/2162-8777/ad1b72.
7. Mabrouk, R.; Naji, H.; Dhahri, H.; Younsi, Z. On Numerical Modeling of Thermal Performance Enhancementof a Heat Thermal Energy Storage System Using a Phase Change Material and a Porous Foam. *Computation* **2022**, *10*, 3, doi:10.3390/computation10010003.
8. Ye, Q.; Deng, Y.; Li, T.; Yu, B.; Sun, D.; Wei, J. Fast Calculation of Latent Heat Storage Process in the Direct Steam Generation Solar Thermal Power System Using a POD Reduced-Order Model. *Solar Energy* **2021**, doi:10.1016/j.solener.2021.09.042.
9. König-Haagen, A.; Faden, M.; Diarce, G. A CFD Results-Based Reduced-Order Model for Latent Heat Thermal Energy Storage Systems with Macro-Encapsulated PCM. *J. Energy Storage* **2023**, *73*, 109235, doi:10.1016/j.est.2023.109235.
10. Xiang, L.; Zhang, B.; Zha, Y.; Xing, G.; Yang, X.; Wang, Z.; Cheng, Y.; Yu, X.; Hu, R.; Luo, X. Physics-Informed Proper Orthogonal Decomposition for Accurate and Superfast Prediction of Thermal Field. *ASME Journal of Heat and Mass Transfer* **2025**, *147*, doi:10.1115/1.4068266.
11. Li, W.; Zhang, Y.; Zhang, X.; Zhao, J. Studies on Performance Enhancement of Heat Storage System with Multiple Phase Change Materials. *J. Energy Storage* **2022**, *47*, doi:10.1016/j.est.2021.103585.
12. Lamrani, B.; Belcaid, A.; Lebrouhi, B.E.; Rhafiki, T. El; Kousksou, T. Numerical Investigation of a Latent Cold Storage System Using Shell-and-Tube Unit. *Energy Storage and Saving* **2023**, *2*, 467–477, doi:10.1016/j.enss.2023.02.008.
13. Tamraparni, A.; Rendall, J.; Shen, Z.; Hun, D.; Shrestha, S. Experimental Investigation on Phase Change Material–Based Finned Tube Heat Exchanger for Thermal Energy Storage and Building Envelope Thermal Management. *Appl. Therm. Eng.* **2025**, *273*, doi:10.1016/j.applthermaleng.2025.126490.
14. Cao, X.; Zhang, N.; Yuan, Y.; Luo, X. Thermal Performance of Triplex-Tube Latent Heat Storage Exchanger: Simultaneous Heat Storage and Hot Water Supply via Condensation Heat Recovery. *Renew. Energy* **2020**, *157*, 616–625, doi:10.1016/j.renene.2020.05.059.
15. Srivastava, U.; Rekha Sahoo, R. Analysis of Energy and Exergy of Eutectic Phase Change Material Solidification for Various Configuration-Based Triplex Tube. *Thermal Science and Engineering Progress* **2024**, *50*, doi:10.1016/j.tsep.2024.102550.

 doi:10.20944/preprints202602.1504.v1

16. El Jemli, R.; Hanchi, N.; Elbahjaoui, R.; Faraji, H. Thermal Analysis of a Triplex-Tube Heat Exchanger System Incorporating Multiple Phase Change Materials. *E3S Web of Conferences* **2025**, *680*, 00143, doi:10.1051/e3sconf/202568000143.
17. Zhang, Q.; Liu, Y.; Yang, Z.; Wang, G.; Lü, X. Investigation of the Thermal Performance of Cascaded Latent Heat Thermal Energy Storage System Based on Composite Phase Change Materials. *International Journal of Exergy* **2023**, *41*, 197–218, doi:10.1504/IJEX.2023.131487.
18. Ait Laasri, I.; Charai, M.; Mghazli, M.O.; Outzourhit, A. Energy Performance Assessment of a Novel Enhanced Solar Thermal System with Topology Optimized Latent Heat Thermal Energy Storage Unit for Domestic Water Heating. *Renew. Energy* **2024**, *224*, 120189, doi:10.1016/j.renene.2024.120189.
19. Taghavi, M.; Ferrantelli, A.; Joronen, T. Multi-Objective Optimization of a Plate Heat Exchanger Thermal Energy Storage with Phase Change Material. *J. Energy Storage* **2024**, *89*, 111645, doi:10.1016/j.est.2024.111645.
20. Gürel, B. Thermal Performance Evaluation for Solidification Process of Latent Heat Thermal Energy Storage in a Corrugated Plate Heat Exchanger. *Appl. Therm. Eng.* **2020**, *174*, 115312, doi:10.1016/j.applthermaleng.2020.115312.
21. Beyne, W.; Johnson, M.; Gutierrez, A.; Paepe, M. De Experimental Validation of a Lower Order Model for a Flat-Plate Latent Thermal Energy Storage Heat Exchanger. *Appl. Therm. Eng.* **2025**, *274*, 126733, doi:10.1016/j.applthermaleng.2025.126733.
22. Park, J.; Shin, D.H.; Lee, S.J.; Shin, Y.; Karng, S.W. Effective Latent Heat Thermal Energy Storage System Using Thin Flexible Pouches. *Sustain. Cities Soc.* **2019**, *45*, 143–150, doi:10.1016/j.scs.2018.10.046.
23. Sharma, A.; Tyagi, V.V.; Chen, C.R.; Buddhi, D. Review on Thermal Energy Storage with Phase Change Materials and Applications. *Renewable and Sustainable Energy Reviews* **2009**, *13*, 318–345, doi:10.1016/j.rser.2007.10.005.
24. Mehling, H.; Cabeza, L.F. *Heat and Cold Storage with PCM*; Springer Berlin Heidelberg: Berlin, Heidelberg, 2008; ISBN 978-3-540-68556-2.
25. Brent, A.D.; Voller, V.R.; Reid, K.J. ENTHALPY-POROSITY TECHNIQUE FOR MODELING CONVECTION-DIFFUSION PHASE CHANGE: APPLICATION TO THE MELTING OF A PURE METAL. *Numerical Heat Transfer* **1988**, *13*, 297–318, doi:10.1080/10407788808913615.
26. Voller, V.R.; Prakash, C. A Fixed Grid Numerical Modelling Methodology for Convection-Diffusion Mushy Region Phase-Change Problems. *Int. J. Heat Mass Transf.* **1987**, *30*, 1709–1719, doi:10.1016/0017-9310(87)90317-6.
27. Lacroix, M. Numerical Simulation of a Shell-and-Tube Latent Heat Thermal Energy Storage Unit. *Solar Energy* **1993**, *50*, 357–367, doi:10.1016/0038-092X(93)90029-N.
28. Dutil, Y.; Rousse, D.R.; Salah, N. Ben; Lassue, S.; Zalewski, L. A Review on Phase-Change Materials: Mathematical Modeling and Simulations. *Renewable and Sustainable Energy Reviews* **2011**, *15*, 112–130, doi:10.1016/j.rser.2010.06.011.
29. Patankar, S. V. *Numerical Heat Transfer and Fluid Flow*; CRC Press, 2018; ISBN 9781315275130.
30. Kunisch, K.; Volkwein, S. Galerkin Proper Orthogonal Decomposition Methods for Parabolic Problems. *Numer. Math. (Heidelb).* **2001**, *90*, 117–148, doi:10.1007/s002110100282.
31. Shakib, M.F.; Scarciotti, G.; Pogromsky, A.Yu.; Pavlov, A.; van de Wouw, N. Model Reduction by Moment Matching with Preservation of Global Stability for a Class of Nonlinear Models. *Automatica* **2023**, *157*, 111227, doi:10.1016/j.automatica.2023.111227.
32. Perev, K. The Unifying Feature of Projection in Model Order Reduction. *Information Technologies and Control* **2014**, *12*, 17–27, doi:10.1515/itc-2016-0003.
33. Mudunuru, M.K.; Karra, S.; Harp, D.R.; Guthrie, G.D.; Viswanathan, H.S. Regression-Based Reduced-Order Models to Predict Transient Thermal Output for Enhanced Geothermal Systems. *Geothermics* **2017**, *70*, 192–205, doi:10.1016/j.geothermics.2017.06.013.
34. Medeiros, R.; Jané, E.; Varas, F.; Higuera, M. Battery Cell Optimisation Using Time– and Parameter–Adaptive Reduced Order Models. *Computers & Mathematics with Applications* **2024**, *161*, 137–154, doi:10.1016/j.camwa.2024.02.043.

 doi:10.20944/preprints202602.1504.v1

35. Rozza, G.; Malik, H.; Demo, N.; Tezzele, M.; Girfoglio, M.; Stabile, G.; Mola, A. Advances in Reduced Order Methods for Parametric Industrial Problems in Computational Fluid Dynamics 2018.
36. Flodén, O.; Persson, K.; Sandberg, G. Reduction Methods for the Dynamic Analysis of Substructure Models of Lightweight Building Structures. *Comput. Struct.* **2014**, *138*, 49–61, doi:10.1016/j.compstruc.2014.02.011.
37. Reddy, S.R.; Freno, B.A.; Cizmas, P.G.A.; Gokaltun, S.; McDaniel, D.; Dulikravich, G.S. Constrained Reduced-Order Models Based on Proper Orthogonal Decomposition. *Comput. Methods Appl. Mech. Eng.* **2017**, *321*, 18–34, doi:10.1016/j.cma.2017.03.038.
38. Shamim, M.B.; Wulfinghoff, S. Variational Three-Field Reduced Order Modeling for Nearly Incompressible Materials. *Comput. Mech.* **2024**, *74*, 1073–1087, doi:10.1007/s00466-024-02468-2.
39. German, P.; Ragusa, J.C. Reduced-Order Modeling of Parameterized Multi-Group Diffusion k-Eigenvalue Problems. *Ann. Nucl. Energy* **2019**, *134*, 144–157, doi:10.1016/j.anucene.2019.05.049.
40. Hay, A.; Borggaard, J.; Akhtar, I.; Pelletier, D. Reduced-Order Models for Parameter Dependent Geometries Based on Shape Sensitivity Analysis. *J. Comput. Phys.* **2010**, *229*, 1327–1352, doi:10.1016/j.jcp.2009.10.033.
41. Manthey, R.; Knospe, A.; Lange, C.; Hennig, D.; Hurtado, A. Reduced Order Modeling of a Natural Circulation System by Proper Orthogonal Decomposition. *Progress in Nuclear Energy* **2019**, *114*, 191–200, doi:10.1016/j.pnucene.2019.03.010.
42. Ramesh, S.S.; Lim, K.M. Reduced-Order Model for Underwater Target Identification Using Proper Orthogonal Decomposition. *J. Sound Vib.* **2017**, *391*, 50–72, doi:10.1016/j.jsv.2016.12.008.
43. Zhuang, Q.; Lorenzi, J.M.; Bungartz, H.-J.; Hartmann, D. Model Order Reduction Based on Runge–Kutta Neural Networks. *Data-Centric Engineering* **2021**, *2*, e13, doi:10.1017/dce.2021.15.
44. Sukuntee, N.; Chaturantabut, S. Parametric Nonlinear Model Reduction Using Machine Learning on Grassmann Manifold with an Application on a Flow Simulation. *J. Nonlinear Sci.* **2024**, *34*, 61, doi:10.1007/s00332-024-10039-1.
45. Ahmed, S.E.; San, O. Forward Sensitivity Analysis and Mode Dependent Control for Closure Modeling of Galerkin Systems. *Computers & Mathematics with Applications* **2023**, *145*, 289–302, doi:10.1016/j.camwa.2023.06.038.
46. Hijazi, S.N.Y.; Freitag, M.; Landwehr, N. POD-Galerkin Reduced Order Models and Physics-Informed Neural Networks for Solving Inverse Problems for the Navier–Stokes Equations 2022.
47. Cicci, L.; Fresca, S.; Manzoni, A. Deep-HyROMnet: A Deep Learning-Based Operator Approximation for Hyper-Reduction of Nonlinear Parametrized PDEs. *J. Sci. Comput.* **2022**, *93*, 57, doi:10.1007/s10915-022-02001-8.
48. Rapún, M.-L.; Terragni, F.; Vega, J.M. Fully Online ROMs and Collocation Based on LUPOD. In; 2020; pp. 81–93.
49. Peng, Z.; Wang, M.; Li, F. A Learning-Based Projection Method for Model Order Reduction of Transport Problems. *J. Comput. Appl. Math.* **2022**, *418*, doi:10.1016/j.cam.2022.114560.
50. Padula, G.; Girfoglio, M.; Rozza, G. A Brief Review of Reduced Order Models Using Intrusive and Non-intrusive Techniques. *PAMM* **2024**, *24*, doi:10.1002/pamm.202400210.
51. Girfoglio, M.; Quaini, A.; Rozza, G. A Linear Filter Regularization for POD-Based Reduced-Order Models of the Quasi-Geostrophic Equations. *Comptes Rendus. Mécanique* **2024**, *351*, 457–477, doi:10.5802/crmeca.183.
52. Mülayim, G. REDUCED ORDER MODELİNG OF BRUSSELATOR MODEL. *International Conference on Modern Problems of Mathematics, Mechanics and their Applications* **2024**, 248, doi:10.58225/mpmma.2024.248.
53. Wang, Q.; Ripamonti, N.; Hesthaven, J.S. Recurrent Neural Network Closure of Parametric POD-Galerkin Reduced-Order Models Based on the Mori-Zwanzig Formalism. *J. Comput. Phys.* **2020**, *410*, 109402, doi:10.1016/j.jcp.2020.109402.
54. Chen, Y.; Ji, L.; Narayan, A.; Xu, Z. L1-Based Reduced Over Collocation and Hyper Reduction for Steady State and Time-Dependent Nonlinear Equations. *J. Sci. Comput.* **2021**, *87*, 10, doi:10.1007/s10915-021-01416-z.
55. Park, J.S.R.; Zhu, X. A Non-Intrusive Bi-Fidelity Reduced Basis Method for Time-Independent Problems. *J. Comput. Phys.* **2024**, *502*, 112797, doi:10.1016/j.jcp.2024.112797.

 doi:10.20944/preprints202602.1504.v1

56. Lee, G.-Y.; Park, K.C.; Park, Y.-H. Reduced-Order Modeling via Proper Generalized Decomposition for Uncertainty Quantification of Frequency Response Functions. *Comput. Methods Appl. Mech. Eng.* **2022**, *401*, 115643, doi:10.1016/j.cma.2022.115643.
57. Vella, C.; Prudhomme, S. PGD Reduced-Order Modeling for Structural Dynamics Applications. *Comput. Methods Appl. Mech. Eng.* **2022**, *402*, 115736, doi:10.1016/j.cma.2022.115736.
58. Ansin, C.; Larsson, F.; Larsson, R. Fast Simulation of 3D Elastic Response for Wheel–Rail Contact Loading Using Proper Generalized Decomposition. *Comput. Methods Appl. Mech. Eng.* **2023**, *417*, 116466, doi:10.1016/j.cma.2023.116466.
59. Dominesey, K.A.; Ji, W. Reduced-Order Modeling of Neutron Transport Eigenvalue Problems Separated in Energy by Proper Generalized Decomposition. *J. Comput. Phys.* **2023**, *486*, doi:10.1016/j.jcp.2023.112137.
60. Yu, J.; Hesthaven, J.S. Model Order Reduction for Compressible Flows Solved Using the Discontinuous Galerkin Methods. *J. Comput. Phys.* **2022**, *468*, 111452, doi:10.1016/j.jcp.2022.111452.
61. Mamonov, A. V.; Olshanskii, M.A. Tensorial Parametric Model Order Reduction of Nonlinear Dynamical Systems. *SIAM Journal on Scientific Computing* **2024**, *46*, A1850–A1878, doi:10.1137/23M1553789.
62. Zappon, E.; Manzoni, A.; Gervasio, P.; Quarteroni, A. A Reduced Order Model for Domain Decompositions with Non-Conforming Interfaces. *J. Sci. Comput.* **2024**, *99*, 22, doi:10.1007/s10915-024-02465-w.
63. Lee, J.; Lee, J.; Cho, H.; Kim, E.; Cho, M. Reduced-Order Modeling of Nonlinear Structural Dynamical Systems via Element-Wise Stiffness Evaluation Procedure Combined with Hyper-Reduction. *Comput. Mech.* **2021**, *67*, 523–540, doi:10.1007/s00466-020-01946-7.
64. Bai, F.; Wang, Y. DEIM Reduced Order Model Constructed by Hybrid Snapshot Simulation. *SN Appl. Sci.* **2020**, *2*, 2165, doi:10.1007/s42452-020-03958-7.
65. Bai, F.; Wang, Y. A Reduced Order Modeling Method Based on GNAT-Embedded Hybrid Snapshot Simulation. *Math. Comput. Simul.* **2022**, *199*, 100–132, doi:10.1016/j.matcom.2022.03.006.
66. Peng, Z.; Wang, M.; Li, F. A Learning-Based Projection Method for Model Order Reduction of Transport Problems. *J. Comput. Appl. Math.* **2023**, *418*, 114560, doi:10.1016/j.cam.2022.114560.
67. Choi, Y.; Coombs, D.; Anderson, R. SNS: A Solution-Based Nonlinear Subspace Method for Time-Dependent Model Order Reduction. *SIAM Journal on Scientific Computing* **2020**, *42*, A1116–A1146, doi:10.1137/19M1242963.
68. Fischer, H.; Roth, J.; Wick, T.; Chamoin, L.; Fau, A. MORe DWR: Space-Time Goal-Oriented Error Control for Incremental POD-Based ROM for Time-Averaged Goal Functionals. *J. Comput. Phys.* **2024**, *504*, doi:10.1016/j.jcp.2024.112863.
69. Lu, H.; Tartakovsky, D.M. Model Reduction via Dynamic Mode Decomposition 2022.
70. Kutz, J.N. Machine Learning Methods for Reduced Order Modeling. In; 2023; pp. 201–228.
71. Alla, A.; Kutz, J.N. Nonlinear Model Order Reduction via Dynamic Mode Decomposition. *SIAM Journal on Scientific Computing* **2017**, *39*, B778–B796, doi:10.1137/16M1059308.
72. Lu, H.; Tartakovsky, D.M. DRIPS: A Framework for Dimension Reduction and Interpolation in Parameter Space. *J. Comput. Phys.* **2023**, *493*, 112455, doi:10.1016/j.jcp.2023.112455.
73. Suh, S.W.; Chung, S.W.; Bremer, P.-T.; Choi, Y. Accelerating Flow Simulations Using Online Dynamic Mode Decomposition 2023.
74. Nedzhibov, G.H. ONLINE DYNAMIC MODE DECOMPOSITION: AN ALTERNATIVE APPROACH FOR LOW RANK DATASETS. *Annals of the Academy of Romanian Scientists Series on Mathematics and Its Application* **2023**, *15*, 229–249, doi:10.56082/annalsarscimath.2023.1-2.229.
75. Beltrán, V.; Le Clainche, S.; Vega, J.M. An Adaptive Data-Driven Reduced Order Model Based on Higher Order Dynamic Mode Decomposition. *J. Sci. Comput.* **2022**, *92*, 12, doi:10.1007/s10915-022-01855-2.
76. Wang, S.; Batool, A.; Sun, X.; Pan, X. Non-Intrusive Reduced-Order Model for Time-Dependent Stochastic Partial Differential Equations Utilizing Dynamic Mode Decomposition and Polynomial Chaos Expansion. *Chaos: An Interdisciplinary Journal of Nonlinear Science* **2024**, *34*, doi:10.1063/5.0200406.
77. Papadopoulos, V.; Soimiris, G.; Giovanis, D.G.; Papadrakakis, M. A Neural Network-Based Surrogate Model for Carbon Nanotubes with Geometric Nonlinearities. *Comput. Methods Appl. Mech. Eng.* **2018**, *328*, 411–430, doi:10.1016/j.cma.2017.09.010.

 doi:10.20944/preprints202602.1504.v1

78. Wu, P.; Qiu, F.; Feng, W.; Fang, F.; Pain, C. A Non-Intrusive Reduced Order Model with Transformer Neural Network and Its Application. *Physics of Fluids* **2022**, *34*, doi:10.1063/5.0123185.
79. Lin, X.; Xiao, D. Parametric Taylor Series Based Latent Dynamics Identification Neural Networks 2024.
80. Simpson, T.; Vlachas, K.; Garland, A.; Dervilis, N.; Chatzi, E. VpROM: A Novel Variational Autoencoder-Boosted Reduced Order Model for the Treatment of Parametric Dependencies in Nonlinear Systems. *Sci. Rep.* **2024**, *14*, 6091, doi:10.1038/s41598-024-56118-x.
81. Zhu, Y.; Sun, Q.; Xiao, D.; Yao, J.; Mao, X. Compressed Neural Networks for Reduced Order Modeling. *Physics of Fluids* **2024**, *36*, doi:10.1063/5.0194598.
82. Jain, M.; Raul, A.; Saha, S.K. Reduced Order Model of Encapsulated PCMs-Based Thermal Energy Storage. In; 2020; pp. 285–295.
83. Experimental Investigation of the Effect of Phase Change Material in Mitigation of Heat. *Aeronautical and Aerospace Engineering* **2024**, *2*, 1–6, doi:10.46632/aae/2/1/1.
84. Singh, M.K.; Sundar, L.S.; Pereira, M.B.; Sousa, A.C.M. Thermal Energy Storage in Phase Change Materials and Its Applications. In *Latent Heat-Based Thermal Energy Storage Systems*; Apple Academic Press: Includes bibliographical references and index., 2020; pp. 29–49.
85. Kumar, S.; Dhingra, S.; Singh, G. A Review of Performance of Thermal Energy Storage System Using PCM in Different Applications. *Int. J. Enhanc. Res. Sci. Technol. Eng.* **2014**, *3*, 287–292.
86. Pernsteiner, D.; Schirrer, A.; Kasper, L.; Hofmann, R.; Jakubek, S. Data-Based Model Reduction for Phase Change Problems with Convective Heat Transfer. *Appl. Therm. Eng.* **2021**, *184*, 116228, doi:10.1016/j.applthermaleng.2020.116228.
87. Blanc, T.J.; Jones, M.R.; Gorrell, S.E.; Duque, E.P.N. Reduced Order Modeling and Compression of Data Produced by Simulations of Transient and Periodic Heat Transfer Processes. *Volume 4: Heat and Mass Transfer Under Extreme Conditions; Environmental Heat Transfer; Computational Heat Transfer; Visualization of Heat Transfer; Heat Transfer Education and Future Directions in Heat Transfer; Nuclear Energy* **2013**, doi:10.1115/ht2013-17604.
88. Feng, L.; Meuris, P.; Schoenmaker, W.; Benner, P. Parametric and Reduced-Order Modeling for the Thermal Analysis of Nanoelectronic Structures. *Mathematics in Industry* **2016**, 155–163, doi:10.1007/978-3-319-30399-4_16.
89. Dermardiros, V. Development Of Reduced-Order Thermal Models Of Building-Integrated Active Pcm-Tes. *ASHRAE TRANSACTIONS, VOL 122, PT 1* **2016**.
90. Stropnik, R.; Koželj, R.; Zavrl, E.; Stritih, U. Improved Thermal Energy Storage for Nearly Zero Energy Buildings with PCM Integration. *Solar Energy* **2019**, *190*, 420–426, doi:10.1016/j.solener.2019.08.041.
91. Zeipel, H.; Frank, T.; Wielitzka, M.; Ortmaier, T. Comparative Study of Model Order Reduction for Linear Parameter-Variant Thermal Systems. In Proceedings of the 2020 IEEE International Conference on Mechatronics and Automation (ICMA); IEEE, October 13 2020; pp. 990–995.
92. Ezzat Khalifa, H.; Koz, M. Phase Change Material Freezing in an Energy Storage Module for a Micro Environmental Control System. *J. Therm. Sci. Eng. Appl.* **2018**, *10*, doi:10.1115/1.4040697.
93. Kashyap, S.; Kabra, S.; Kandasubramanian, B. Graphene Aerogel-Based Phase Changing Composites for Thermal Energy Storage Systems. *J. Mater. Sci.* **2020**, *55*, 4127–4156, doi:10.1007/s10853-019-04325-7.
94. Ran, F.; Chen, Y.; Cong, R.; Fang, G. Flow and Heat Transfer Characteristics of Microencapsulated Phase Change Slurry in Thermal Energy Systems: A Review. *Renewable and Sustainable Energy Reviews* **2020**, *134*, 110101, doi:10.1016/j.rser.2020.110101.
95. Su, W.; Darkwa, J.; Zhou, T.; Du, D.; Kokogiannakis, G.; Li, Y.; Wang, L.; Gao, L. Development of Composite Microencapsulated Phase Change Materials for Multi-Temperature Thermal Energy Storage. *Crystals (Basel).* **2023**, *13*, 1167, doi:10.3390/cryst13081167.
96. Md Ahsan Habib; Muhammad Mustafizur Rahman Phase Change Materials for Applications in Building Thermal Energy Storage (Review). *Thermal Engineering* **2024**, *71*, 649–663, doi:10.1134/S0040601524700174.
97. Kim, S.; Yang, T.; Miljkovic, N.; King, W.P. Phase Change Material Integrated Cooling for Transient Thermal Management of Electronic Devices. *Int. J. Heat Mass Transf.* **2023**, *213*, 124263, doi:10.1016/j.ijheatmasstransfer.2023.124263.

 doi:10.20944/preprints202602.1504.v1

98. Hua, W.; Lv, X.; Zhang, X.; Ji, Z.; Zhu, J. Research Progress of Seasonal Thermal Energy Storage Technology Based on Supercooled Phase Change Materials. *J. Energy Storage* **2023**, *67*, 107378, doi:10.1016/j.est.2023.107378.
99. Hu, Y.; Guo, R.; Heiselberg, P.K.; Johra, H. Modeling PCM Phase Change Temperature and Hysteresis in Ventilation Cooling and Heating Applications. *Energies (Basel).* **2020**, *13*, 6455, doi:10.3390/en13236455.
100. Nokhosteen, A.; Sobhansarbandi, S. Melting Behavior Prediction of Latent Heat Storage Materials: A Multi-Pronged Solution. *J. Energy Storage* **2023**, *65*, 107018, doi:10.1016/j.est.2023.107018.
101. N., L.N. Assessment of Latent Heat Thermal Storage Systems Operating with Multiple Phase Change Materials. *J. Energy Storage* **2019**, *23*, 442–455, doi:10.1016/j.est.2019.04.008.
102. Michael Shanks Uduak Inyang-Udoh, N.J. Design and Validation of a State-Dependent Riccati Equation Filter for State of Charge Estimation in a Latent Thermal Storage Device. *ASM International* **2023**, doi:https://doi.org/10.1115/1.4062707.
103. Raghavendra Rohith Kasibhatla Andreas Knig-Haagen, D.B. Numerical Modelling of Wetting Phenomena During Melting of PCM. *Elsevier BV* **2016**, doi:https://doi.org/10.1016/j.proeng.2016.08.349.
104. Tripathi, P.M.; Marconnet, A.M. A New Thermal Management Figure of Merit for Design of Thermal Energy Storage with Phase Change Materials. *Int. J. Heat Mass Transf.* **2024**, *220*, 124952, doi:10.1016/j.ijheatmasstransfer.2023.124952.
105. Naresh Kumar Goud Ranga S. Gugulothu, P.G. Thermal Optimization of Latent Heat Energy Storage Through Fin Geometry Natural Convection and PCM Properties for Superior Phase Change Performance. *Heat Transfer* **2025**, doi:10.1002/htj.23374.
106. Mallya, N.; Haussener, S. Buoyancy-Driven Melting and Solidification Heat Transfer Analysis in Encapsulated Phase Change Materials. *Int. J. Heat Mass Transf.* **2021**, *164*, 120525, doi:10.1016/j.ijheatmasstransfer.2020.120525.
107. Liu, S.; Li, Y.; Zhang, Y. Mathematical Solutions and Numerical Models Employed for the Investigations of PCMs' Phase Transformations. *Renewable and Sustainable Energy Reviews* **2014**, *33*, 659–674, doi:10.1016/j.rser.2014.02.032.
108. Chernov, A.A.; Pil'nik, A.A. Gas Segregation during Crystallization Process. *Int. J. Heat Mass Transf.* **2018**, *119*, 963–969, doi:10.1016/j.ijheatmasstransfer.2017.12.003.
109. Liu, S.; Li, Y.; Zhang, Y. Review on Heat Transfer Mechanisms and Characteristics in Encapsulated PCMs. *Heat Transfer Engineering* **2014**, *36*, 880–901, doi:10.1080/01457632.2015.965093.
110. Sakakini, T.J.; Koeln, J.P. Switched Moving Boundary Modeling of Phase Change Thermal Energy Storage Systems. In Proceedings of the 2023 IEEE Conference on Control Technology and Applications (CCTA); IEEE, August 16 2023; pp. 941–947.
111. Van Riet, V.; Shockner, T.; Beyne, W.; Ziskind, G.; De Paepe, M.; Degroote, J. Limitations of the Enthalpy-Porosity Method for Numerical Simulation of Close-Contact Melting on Inclined Surfaces. *J. Phys. Conf. Ser.* **2024**, *2766*, 012214, doi:10.1088/1742-6596/2766/1/012214.
112. R. Santiago-Acosta E. Hernndez-Cooper, R.P.J.O. Effects of Volume Changes on the Thermal Performance of PCM Layers Subjected to Oscillations of the Ambient Temperature: Transient and Steady Periodic Regimes. *Molecules* **2022**, doi:10.3390/molecules27072158.
113. Sarath, K.P.; Feroz Osman, M.; Mukhesh, R.; Manu, K. V; Deepu, M. A Review of the Recent Advances in the Heat Transfer Physics in Latent Heat Storage Systems. *Thermal Science and Engineering Progress* **2023**, *42*, 101886, doi:10.1016/j.tsep.2023.101886.
114. Zhang, C.; Zhang, X.; Qiu, L.; Zhao, Y. Thermodynamic Investigation of Cascaded Latent Heat Storage System Based on a Dynamic Heat Transfer Model and DE Algorithm. *Energy* **2020**, *211*, 118578, doi:10.1016/j.energy.2020.118578.
115. Luke G. Min H. Kwon, S.V.X.B.M.A.K.E.G. Thermal Management of 3D Chips and Monolithic Integrated Circuits Using Phase Change Materials - Si/Cu Composites. *J. Electron. Packag.* **2025**, doi:10.1115/1.4070160.
116. Brendan Gillis, N.J. Numerical Validation of Effective Specific Heat Functions for Simulating Melting Dynamics in Latent Heat Thermal Energy Storage Modules. *Intersociety Conference on Thermal and Thermomechanical Phenomena in Electronic Systems* **2021**, doi:10.1109/ITherm51669.2021.9503136.

 doi:10.20944/preprints202602.1504.v1

117. Zayed, M.E.; Zhao, J.; Li, W.; Elsheikh, A.H.; Elbanna, A.M.; Jing, L.; Geweda, A.E. Recent Progress in Phase Change Materials Storage Containers: Geometries, Design Considerations and Heat Transfer Improvement Methods. *J. Energy Storage* **2020**, *30*, 101341, doi:10.1016/j.est.2020.101341.
118. Kenisarin, M.M.; Mahkamov, K.; Costa, S.C.; Makhkamova, I. Melting and Solidification of PCMs inside a Spherical Capsule: A Critical Review. *J. Energy Storage* **2020**, *27*, 101082, doi:10.1016/j.est.2019.101082.
119. Chibani, A.; Dehane, A.; Merouani, S.; Bougriou, C.; Guerraiche, D. Melting/Solidification of Phase Change Material in a Multi-Tube Heat Exchanger in the Presence of Metal Foam: Effect of the Geometrical Configuration of Tubes. *Energy Storage and Saving* **2022**, *1*, 241–258, doi:10.1016/j.enss.2022.07.004.
120. Meftah Uddin A. S. Virk, C.P. Natural Convection in the Melting of PCM in a Cylindrical Thermal Energy Storage System: Effects of Flow Arrangements of Heat Transfer Fluid and Associated Thermal Boundary Conditions. *Journal of Thermal Science and Engineering Apllications* **2023**, doi:10.1115/1.4063045.
121. Rui Yang C. Howland, H.L.R.V.D.L. Enhanced Efficiency of Latent Heat Energy Storage by Inclination. *PRX Energy* **2024**, doi:10.1103/prxenergy.3.043006.
122. Abreha, B.G.; Mahanta, P.; Trivedi, G. Performance Improvement Techniques in Shell-and-Tube Type of LHS Unit. *Lecture Notes in Mechanical Engineering* **2021**, 153–163, doi:10.1007/978-981-16-3497-0_12.
123. Hasnain, F. ul; Irfan, M.; Khan, M.M. Branching of Fins and Addition of Al2O3 Nanoparticles for Rapid Charging and Discharging of Latent Heat Storage Unit. *Int. J. Energy Res.* **2022**, *46*, 22625–22640, doi:10.1002/er.8565.
124. Mulani Feroz Osman, M.D. EFFECTS OF RAPID BOUNDARY HEAT FLUX FLUCTUATIONS ON WAVY HEAT TRANSFERRING SURFACES IN LATENT ENERGY STORAGES. *Journal of Thermal Science and Engineering Apllications* **2025**, doi:10.1115/1.4068343.
125. Tao, Y.B.; Carey, V.P. Effects of PCM Thermophysical Properties on Thermal Storage Performance of a Shell-and-Tube Latent Heat Storage Unit. *Appl. Energy* **2016**, *179*, 203–210, doi:10.1016/j.apenergy.2016.06.140.
126. Shen, S.; Wu, C.; Duan, F. Machine Learning for Predicting the PCM Melting Process in a Rectangular Enclosure Energy Storage. *AI Thermal Fluids* **2025**, *1*, 100001, doi:10.1016/j.aitf.2024.100001.
127. Yan, P.; Wen, C.; Ding, H.; Wang, X.; Yang, Y. The Potential of Machine Learning to Predict Melting Response Time of Phase Change Materials in Triplex-Tube Latent Thermal Energy Storage Systems. *Appl. Energy* **2025**, *390*, doi:10.1016/j.apenergy.2025.125863.
128. Tomasetto, M.; Manzoni, A.; Braghin, F. Real-Time Optimal Control of High-Dimensional Parametrized Systems by Deep Learning-Based Reduced Order Models. **2024**, doi:10.1016/j.cma.2025.118030.
129. Lu, Y.; Chi, B.; Zuo, H.; Xu, H.; Zeng, K.; Gao, J.; Yang, H.; Chen, H. Heat Transfer Enhancement of Latent Heat Thermal Energy Storage with Longitudinal Stepped Fins inside Heat Transfer Fluid. *J. Energy Storage* **2024**, *87*, 111546, doi:10.1016/j.est.2024.111546.
130. Dai, H.; Wang, Y.; Wang, N.; Li, H.; Gao, M. Simulation Study on Charging Performance of the Latent Energy Storage Heat Exchanger with a Novel Conical Inner Tube. *J. Energy Storage* **2022**, *56*, 106006, doi:10.1016/j.est.2022.106006.
131. Wang, Y.; Zadeh, P.G.; Duong, X.Q.; Chung, J.D. Optimizing Fin Design for Enhanced Melting Performance in Latent Heat Thermal Energy Storage Systems. *J. Energy Storage* **2023**, *73*, 109108, doi:10.1016/j.est.2023.109108.
132. Lakhani, S.; Raul, A.; Saha, S.K. Dynamic Modelling of ORC-Based Solar Thermal Power Plant Integrated with Multitube Shell and Tube Latent Heat Thermal Storage System. *Appl. Therm. Eng.* **2017**, *123*, 458–470, doi:10.1016/j.applthermaleng.2017.05.115.
133. Kang, Y.; Zhang, Y.; Jiang, Y.; Zhu, Y. GENERAL MODEL OF ANALYZING THE THERMAL PERFORMANCE OF LATENT HEAT THERMAL ENERGY STORAGE SYSTEMS WITH VARIOUS PCM CAPSULES. In Proceedings of the Proceeding of Proceedings of Symposium on Energy Engineering in the 21st Century (SEE2000) Volume I-IV; Begellhouse: Connecticut, 2023; pp. 788–795.
134. Isania, F.; Galgaro, A. Machine Learning for Design Optimization and PCM-Based Storage in Plate Heat Exchangers: A Review. *Energies (Basel).* **2025**, *18*, 5115, doi:10.3390/en18195115.
135. Eze, V.H.U.; Tamball, J.S. Advanced Modeling Approaches for Latent Heat Thermal Energy Storage Systems. *IAA Journal of Applied Sciences* **2024**, *11*, 49–56, doi:10.59298/IAAJAS/2024/6.68.39.34.

 doi:10.20944/preprints202602.1504.v1

136. Crespo, A.; Barreneche, C.; Ibarra, M.; Platzer, W. Latent Thermal Energy Storage for Solar Process Heat Applications at Medium-High Temperatures – A Review. *Solar Energy* **2019**, *192*, 3–34, doi:10.1016/j.solener.2018.06.101.
137. Opolot, M.; Zhao, C.; Liu, M.; Mancin, S.; Bruno, F.; Hooman, K. A Review of High Temperature (>=500 °C) Latent Heat Thermal Energy Storage. *Renewable and Sustainable Energy Reviews* **2022**, *160*, 112293, doi:10.1016/j.rser.2022.112293.
138. Zou, B.; Peng, J.; Li, S.; Li, Y.; Yan, J.; Yang, H. Comparative Study of the Dynamic Programming-Based and Rule-Based Operation Strategies for Grid-Connected PV-Battery Systems of Office Buildings. *Appl. Energy* **2022**, *305*, 117875, doi:10.1016/j.apenergy.2021.117875.
139. Shabgard, H.; Song, L.; Zhu, W. Heat Transfer and Exergy Analysis of a Novel Solar-Powered Integrated Heating, Cooling, and Hot Water System with Latent Heat Thermal Energy Storage. *Energy Convers. Manag.* **2018**, *175*, 121–131, doi:10.1016/j.enconman.2018.08.105.
140. Abdelgaied, M.; Kabeel, A.E.; Sathyamurthy, R. Improving the Performance of Solar Powered Membrane Distillation Systems Using the Thermal Energy Storage Mediums and the Evaporative Cooler. *Renew. Energy* **2020**, *157*, 1046–1052, doi:10.1016/j.renene.2020.05.123.
141. Tomassetti, S.; Aquilanti, A.; Muciaccia, P.F.; Coccia, G.; Mankel, C.; Koenders, E.A.B.; Di Nicola, G. A Review on Thermophysical Properties and Thermal Stability of Sugar Alcohols as Phase Change Materials. *J. Energy Storage* **2022**, *55*, 105456, doi:10.1016/j.est.2022.105456.
142. Zhao, Y.; Zhao, C.Y.; Markides, C.N.; Wang, H.; Li, W. Medium- and High-Temperature Latent and Thermochemical Heat Storage Using Metals and Metallic Compounds as Heat Storage Media: A Technical Review. *Appl. Energy* **2020**, *280*, 115950, doi:10.1016/j.apenergy.2020.115950.
143. Achkari, O.; El Fadar, A. Latest Developments on TES and CSP Technologies – Energy and Environmental Issues, Applications and Research Trends. *Appl. Therm. Eng.* **2020**, *167*, 114806, doi:10.1016/j.applthermaleng.2019.114806.